Dominik Amschl, BSc

Measurement and compensation of mm-wave IQ-Mixers for Radar applications

Master's Thesis

to achieve the university degree of

Master of Science

Master's degree programme: Electrical Engineering

Submitted to

Graz University of Technology

Supervisor
Ass.Prof. Dipl.-Ing. Dr.techn. Michael Gadringer
Institute of Microwave and Photonic Engineering

Graz, March 2021

Table of content

List of Figures

AFFIDAVIT

I declare that I have authored this thesis independently, that I have not used other than the declared sources/resources, and that I have explicitly indicated all material which has been quoted either literally or by content from the sources used. The text document uploaded to TUGRAZonline is identical to the present master's thesis dissertation.

Date Signature

Zusammenfassung

Seit der Massenproduktion des PKWs durch Henry Ford sind jedes Jahr mehr Fahrzeuge auf den Straßen unterwegs. Die Sicherheit und Zuverlässigkeit der Fahrzeuge wurde konstant weiterentwickelt. Die meisten Sicherheitssysteme in einem PKW wie Knautschzonen, Sicherheitsgurte oder Airbags schützen den Fahrer im Falle eines Unfalls, verhindern diesen aber nicht. Dank der ständigen Weiterentwicklung im Bereich der Halbleiterelektronik werden aktive Systeme wie Hinderniserkennung und Notbremssysteme immer beliebter und werden bald in jedem PKW zu finden sein. Der zentrale Teil solcher Systeme ist fast immer ein Radar, welches im Frontbereich des Fahrzeugs montiert ist. Es sendet periodisch Funkwellen aus und empfängt die reflektierten Echos. Daraus lässt sich eine sehr gute Abbildung der Umgebung erstellen. Diese Abbildung kann vom Boardcomputer für Komfort- und Notsysteme verwendet werden. Da es sich hierbei um sicherheitsrelevante Systeme handelt, muss auch das Radar als wichtiger Sensor nach sehr strengen Auflagen entwickelt und getestet werden. Moderne Radarsysteme für den Automobilbereich bestehen oft nur mehr aus einer Stromversorgung, einem Mikrocontroller und einem Radarchip. Der Radarchip ist verantwortlich für das Senden, Empfangen und Verarbeiten aller notwendigen Signale. Diese Funktionalität muss bereits während der Entwicklung des Chips sehr genau geprüft werden. Eine sehr wichtige Prüfung ist, ob der Chip auch wirklich als Radar funktioniert. Dafür wird in einem Labor der Chip mit einem sehr speziellen und aufwendigen Testsystem verbunden. Dieses Testsystem, ein Radarzielsimulator, ist in der Lage das gesendete Signal des Radars so zu verändern, wie es z.B. ein Fußgänger auf der Straße machen würde. Das veränderte Signal wird zurück ins Radar geführt und ausgewertet. Ein solcher Zielsimulator ist sehr aufwändig und teuer. Ziel dieser Arbeit ist es ein wesentlich einfacheres Bauteil, einen IQ-Mixer, zu verwenden, um ähnliche Ergebnisse zu erreichen. Dafür müssen diverse ungewünschte Effekte des IQ-Mixers ermittelt und kompensiert werden.

Diese Masterarbeit wurde am Institut für Hochfrequenztechnik der Technischen Universität Graz verfasst und mit Kooperation der Firma Infineon Technologies Austria AG in Graz entwickelt.

Abstract

Since the mass production of the automobile by Henry Ford the number of cars on the streets is increasing year over year. The safety and reliability of cars has also increased steadily with each new generation. Most safety systems are still passive like crumble zones, seat belts or air bags which help a lot in reducing injuries during an accident but they don't actively prevent anything. Semiconductor electronics have become even more advanced and are now allowing the implementation of active systems like obstacle detection or emergency breaking. The central part of such systems is often a Radar mounted in the front of the car. The Radar emits radio waves and listens for the echo created by the surrounding environment. The echo allows for the creation of a detailed enough image of everything in front of the car. This image can then be used for comfort or safety features by the main computer of the car. Such safety systems have to follow special rules during development to ensure that it works reliable and predictable. Modern automotive Radars use a single chip for generating, receiving and processing all necessary signals. This chip must also follow all safety rules during development and needs to be tested extensively to guaranty all requirements are met. A very important test is to see if the chip works as a Radar. For this test the chip is connected to a Radar Target Stimulator (RTS) in a lab environment. The RTS is capable of receiving the signals send out by the Radar and change them in a way a pedestrian or car on the street would do. The modified signals are fed back into the Radar and analysed. All that needs to be done in real time since electromagnetic waves propagate through air at the speed of light. That makes a RTS a very powerful but expensive piece of equipment. Goal of this thesis is to use an IQ-Mixer instead of a RTS to achieve similar results. To do so a number of unwanted effects of the IQ-Mixer must be characterized and compensated.

This Master thesis has be written on the Institute of microwave and photonic engineering at Graz University of technology in cooperation with Infineon Technologies Austria AG in Graz.

1. Introduction

1.1. Motivation: Automotive Radar and Radar Target Stimulation

Modern cars provide more features and safety with every new model. Adaptive cruise control, emergency breaks and even some form of automated driving are already a reality [1]. To be able to offer those functions the main computer or control unit inside a car must understand the environment around the car [2]. To get this information into the digital domain for the computer a lot of different sensors are used. For the scope of this thesis only the sensors that give the computer some sort of vision of the surrounding area are important, specifically Radars and cameras. An easy to understand sensor is a normal optical camera. It can give a detailed information on its surrounding, since it uses the same principle as a human eye and our wold is built to be seen by human eyes. At first, a camera seems to be the perfect candidate to let the computer "see" the real world, but there are a lot of drawbacks as well. A camera needs light either from a natural source like the sun or an artificial source like headlamps. Not enough or even too much light will reduce the amount of useful information that can be gathered. This also makes it very dependent on the weather and a tiny piece of dirt could be enough to blind it. The huge amount of information also doesn't come for free and needs a lot of computing power. Another big drawback is the limited range and if you want to evaluate the distance to an object the system usually needs more than one camera to capture a 3D image. For all those reasons an optical system is still only found in conjunction with an automotive Radar [3].

The term Radar stands for Radio detection and ranging [4]. The basic principle of a Radar is very simple and was first used before the Second World War so nearly 100 years ago. A Radar sends out an electromagnetic pulse and listens for an echo of that pulse. The frequency, the shape of the pulse, the power and the antennas of the system can vary a lot and all have different impacts on the performance of the Radar. Modern Radars also have built-in signal processing that is able to detect and classify obstacles like cars, pedestrians and walls. Those detected obstacles are called targets. This is done to reduce the amount of data that has to be send to the board computer. A very simple and often used way to describe a target seen by the Radar uses only three characteristics of the target. The relative speed $\mathbf{v_r}$ ($= v_2 - v_1$) between the Radar and the target, the distance **d** between the Radar and the target and the amount of reflected power from the target. The last parameter is called the Radar cross section **RCS** and it is a synthetic number to compare the reflectivity as well as size and shape of different targets.

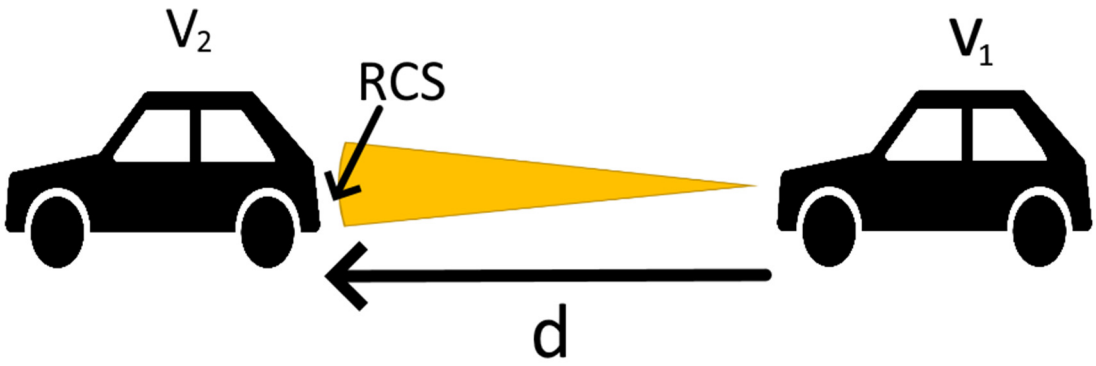

Figure 1: Simplified automotive radar scenario

During the development of the car or even just the Radar itself, it is necessary to test every part of the system and verify its functionality. In later stages of the development, these tests can be carried out on a special road with controlled targets and obstacles. The drawback of those tests is the required effort and the huge costs to setup the environment. Repeatability is also an important topic and debugging can be hard if you have real cars driving at highway speeds. For all those reasons it is desirable to be able to perform the tests in a more controllable and repeatable way [5]. A commonly used device to achieve this is called a Radar Target Stimulator or short RTS. It is placed in front of the Radar, receives the signals from the Radar, alters the signal accordingly and sends the response back to the Radar. With such a system it is possible to test a Radar system without the need to move anything and it can be done in a very repeatable way in a lab. To be able to do all those things the RTS must be capable of changing the signal from the Radar in real time since the transmitted electromagnetic wave and its echo are propagating at light speed and the distance to a target is calculated by measuring the delay of the reflected echo. Every additional delay introduced by the RTS because of additional cables or signal processing steps will show up as additional distance to the target. One way of doing all this is by first converting the frequency of the signal down to a much lower range, sampling it with an analogue to digital converter, digitally process the signal in an FPGA, converting it back into an analogue signal and last converting the frequency back up again before it is send back. Other ways to achieve the same goal could be by physically delaying the signal either with long transmission lines or going through an optical system which applies long glass fibres. All of those steps require very expensive components and a fully capable RTS can cost upwards of 100 k€ [6]. A lot of tests however don't need the full range of features from a modern RTS. In the development of the Radar it is already very helpful to just have the possibility to delay the signal between to receive and transmit parts. This can be done by a simple delay line. This delay line is still expensive but a lot cheaper than a RTS. The drawback of a delay line is its fixed delay. If another distance is needed then another delay line has to be used. In case of an FMCW radar the delay between the received and transmitted signal causes a small shift in frequency of the received signal since it is just a past version of the modulated transmitted signal. A detailed explanation about this can be found in Chapter 2.6. To emulate a target under these conditions it is sufficient to shift the transmitted signal of the Radar a bit in frequency and send it back. This is again explained in Chapter 2.6. Shifting a frequency is achieved by a process called mixing. A Mixer takes two signals and creates both the sum and the difference in frequency of the two original

signals. See Chapter 2.1 for a detailed explanation about Mixers. By combining two Mixers it is possible to create a Mixer that only generates the sum or the difference in frequency depending on the input signals. These types of Mixers are called IQ-Mixers or IQ-modulators and are described in Chapter 2.2. The goal if this Theses is to use an off-the-shelf IQ-Mixer to shift the frequency of a Radar in the same way as a distant target would to. To be able to achieve this functionality in practice a lot of unwanted effects of the Mixer (see Chapter 2.3) must be considered and compensated in a further step with the help of predistortion techniques (Chapter 2.4).

The next major chapter will go over all the necessary theory. This includes the basic functionality of a frequency Mixer (chapter 2.1) which will be refined into the ideal behaviour of an IQ-Mixer (chapter 2.2). Afterwards an explanation of all the unwanted effects split into linear (Chapter 2.3.1) and nonlinear (Chapter 2.3.2) effects of a real IQ-Mixer (Chapter 2.3) will be given. How those effects will be compensated by predistorting the input signal is part of Chapter 2.4. To get an understanding of how a Radar is working the basic principle is explained in Chapter 2.5 and more details of an FMCW-Radar is given in Chapter 2.6. A brief explanation on a common interpretation of the resulting data from a Radar using the so-called Range-Doppler-Map is presented in Chapter 2.7.

An overview on the measurement campaign to characterize the IQ-Mixer starts in Chapter 3 by a description of the setup and the device under test. These measurements are divided into the different groups that were performed to incrementally gain more and more insight into the device under test and to achieve a better performance with every step. In Chapter 4.7 the final result measured with a Radar system is presented.

Chapter 6 discusses the limitations of the found results before Chapter 7 draws a conclusion and highlights possible future improvements.

2. Theory

2.1. Frequency Mixers

A Mixer consists of a circuit with nonlinear behaviour that is used to create new frequencies from two input signals. [7]

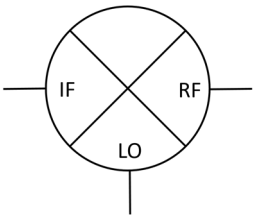

Figure 2: Mixer symbol

A Mixer is usually driven by a signal from a generator called the Local oscillator (LO) with rather high power. The second signal contains the information that gets modulated onto the LO and is called the input- or intermediate frequency (IF) signal. The output or radio frequency (RF) signal contains both the sum and the difference of the two input signals at the same time. These two parts of the output signal are also called the upper sideband (USB) and the lower sideband (LSB). A part of the original LO is also present at the output due to technical limits in the construction. If the Mixer is used in this way to modulate a lower signal onto a higher one it can also be called a modulator. Most Mixers can be used for both up converting/modulating and down converting/demodulating a signal. Most commercially available device are built to perform better in one of those modes.

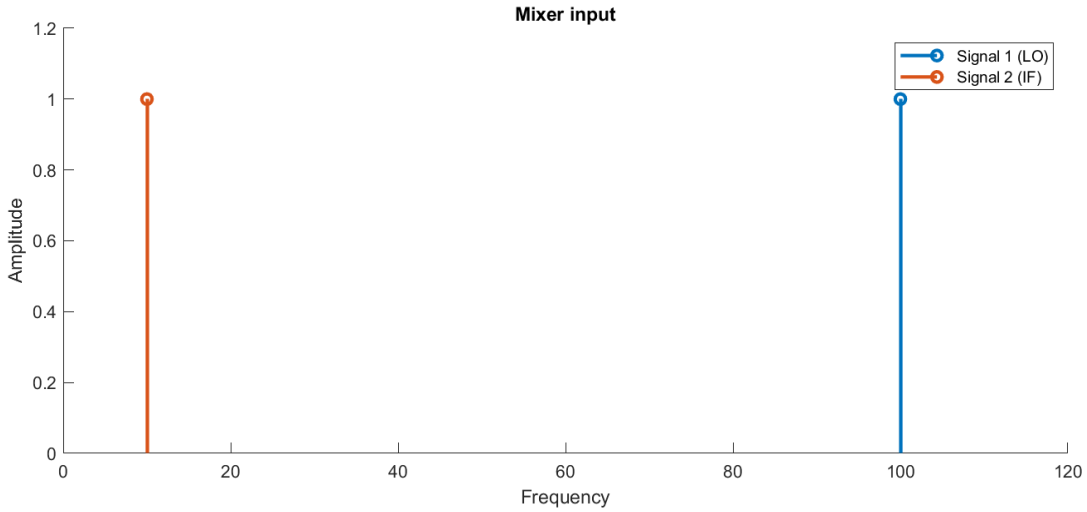

Figure 3: Mixer input signals

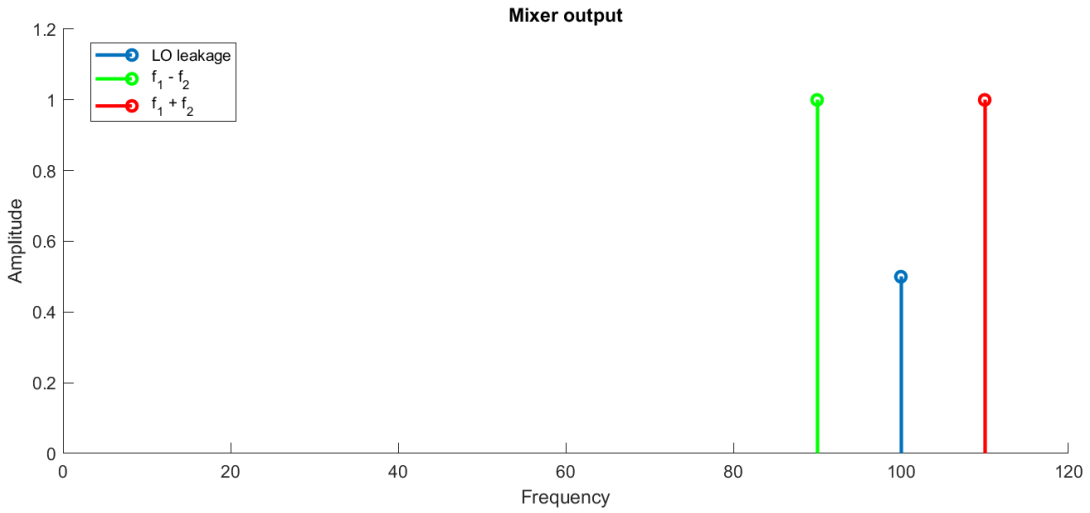

Figure 4: Resulting signals at Mixer output

The simplest form of a mixing circuit is a diode. An ideal diode is described with the following formula [8]:

$$I = I_S(e^{\frac{qV}{nkT}} - 1) \tag{1}$$

$I \dots Current\ flowing\ through\ the\ diode$
$I_S \dots Reverse\ saturation\ current$
$q \dots elementary\ charge\ of\ an\ electron$
$V \dots Voltage\ across\ the\ diode$
$n \dots ideality\ factor$
$k \dots Boltzmann\ constant$
$T \dots absolute\ temperature$

This exponential function can be expanded and approximated by a second order Taylor series expansion:

$$e^x - 1 \approx x + \frac{x^2}{2} \tag{2}$$

Now, the sum of two input signals $v_1 + v_2$ is applied to the diode and the resulting current is converted into a voltage again. Additionally, all constant factors and higher order terms are ignored. Then the output will have the form:

$$V_{out} = (v_1 + v_2) + \frac{1}{2}(v_1 + v_2)^2 \tag{3}$$

If the input signals are now sinusoidal with $v_1 = \sin \omega_1 t$ and $v_2 = \sin \omega_2 t$ the output becomes:

$$V_{out} = (\sin \omega_1 t + \sin \omega_2 t\ ) + \frac{1}{2}(\sin \omega_1 t + \sin \omega_2 t\ )^2 \tag{4}$$

The quadratic term can be expanded:

$$V_{out} = (\sin \omega_1 t + \sin \omega_2 t\ ) + \frac{1}{2}(\sin^2 \omega_1 t + 2 \sin \omega_1 t * \sin \omega_2 t + \sin^2 \omega_2 t) \quad (5)$$

Ignoring everything except the part that has both frequencies multiplied $\sin \omega_1 t * \sin \omega_2 t$ and using the product to sum identity (6)

$$\sin \alpha * \sin \beta = \frac{1}{2}(\cos(\alpha - \beta) - \cos(\alpha + \beta)) \quad (6)$$

The resulting signal will have both the sum and the difference of the two input frequencies:

$$V_{out} = \cos((\alpha - \beta)\ t) - \cos((\alpha + \beta) t) \quad (7)$$

2.2. Ideal IQ-Mixers

A normal Mixer always generates both the upper sideband and the lower sideband simultaneously. If a Mixer is used as a frequency converter like the one discussed in this Theses one sideband is unwanted. In telecommunication systems, this problem is solved by building a multi stage system with two or more Mixers and choosing the frequencies of each stage so that the unwanted sideband can be filtered out before the signal is fed to the next stage. Another way to get rid of the unwanted sideband is the use of a single sideband Mixer or an IQ-Mixer that is driven to be a single sideband Mixer. An IQ-Mixer consists of two identical normal Mixers. The RF outputs of both Mixers are simply combined by a combining network. The LO input for each Mixer is provided from the same source and is split by a 90° hybrid splitting network. This network splits the incoming signal equally between both outputs but one output gets an additional 90° shift in phase. The Mixer that gets the LO without any change is called the in-phase (I) Mixer. The Mixer with the additional 90° phase on the LO is called the quadrature (Q) Mixer. [9]

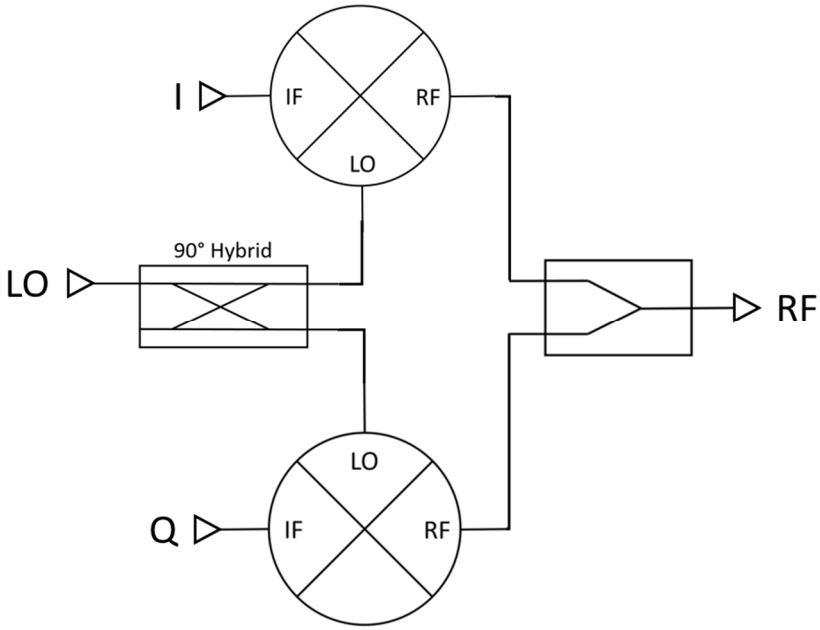

Figure 5: Block diagram of an ideal IQ-Mixer

This configuration allows the user to change each sideband individually if the IQ-Mixer is driven correctly. To use this Mixer as a single sideband Mixer the I and Q input have to receive the same signal but one of the inputs needs to be shifted by an additional 90° in phase. Which input is shifted in phase determines which sideband is made available. To prove this behaviour we start with Euler's formula:

$$\cos(\omega t) = \frac{e^{j\omega t} + e^{-j\omega t}}{2}$$
$$\sin(\omega t) = \frac{-je^{j\omega t} + je^{-j\omega t}}{2} \qquad (8)$$

The I input signal is any time dependent signal

$$a(t) \tag{9}$$

The LO drive for the I Mixer is a cosine signal expressed as

$$\frac{e^{j\omega t} + e^{-j\omega t}}{2} \tag{10}$$

The upconverted signal from the I Mixer is then

$$\frac{e^{j\omega t} + e^{-j\omega t}}{2} a(t) \tag{11}$$

For the Q Mixer the input signal is the same but shifted by 90°

$$j * a(t) \tag{12}$$

The LO for the Q Mixer is also shifted by 90° because of the hybrid power splitter and therefore a sinusoidal signal

$$\frac{-je^{j\omega t} + je^{-j\omega t}}{2} \tag{13}$$

The upconverted signal from the Q Mixer is

$$\frac{-je^{j\omega t} + je^{-j\omega t}}{2} j * a(t) \tag{14}$$

Both signals are now combined by the power combiner

$$\begin{aligned} &\frac{e^{j\omega t} + e^{-j\omega t}}{2} a(t) + \frac{-je^{j\omega t} + je^{-j\omega t}}{2} j * a(t) = \\ &= \frac{1}{2} a(t)\left(e^{j\omega t} + e^{-j\omega t} + e^{j\omega t} - je^{-j\omega t}\right) = \\ &= a(t) * e^{j\omega t} \end{aligned} \tag{15}$$

The result is the input signal modulated only onto the upper sideband. The lower sideband got cancelled out by this operation. If the input signal is a simple sinusoidal with one frequency f_2 and the LO is another signal with frequency f_1 the output of this Mixer is the LO frequency plus the IF frequency $f_2 + f_1$. For this thesis the LO frequency needs to be moved to a lower frequency so the phase of the I- and Q-input signals is chosen to get the lower sideband instead of the upper one.

2.3. Real IQ-Mixers

The previous chapter described the ideal behaviour of an IQ-Mixer. A real device is never perfect and has a number of properties that are not wanted. These properties can be grouped into linear and nonlinear effects. Linear effects occur as the used components do not fulfil the assumptions that the signals are perfectly the same with a perfect 90° in phase shift. They don't alter the input signals in frequency but cause problems with the single sideband upconversion. Nonlinear effects can change the input signal and mainly cause harmonics and intermodulation distortion. [10]

2.3.1. Phase and Gain Imbalance

Both phase and gain imbalance can come from any part of the system like a hybrid power splitter that doesn't divide the power equally or applies a slightly different phase to one of the branches. If the two Mixers are not matched perfectly this can also have similar effect. Since the device is treated like a black box and the errors are linear it doesn't matter were the imbalances originate. The phase error of both branches is added together, called phase imbalance and is associated to one branch of the IQ-Mixer. The same is done for the gain. One branch is treated is ideal with a gain of one and the other branch gets associated with the combined gain error of both branches.

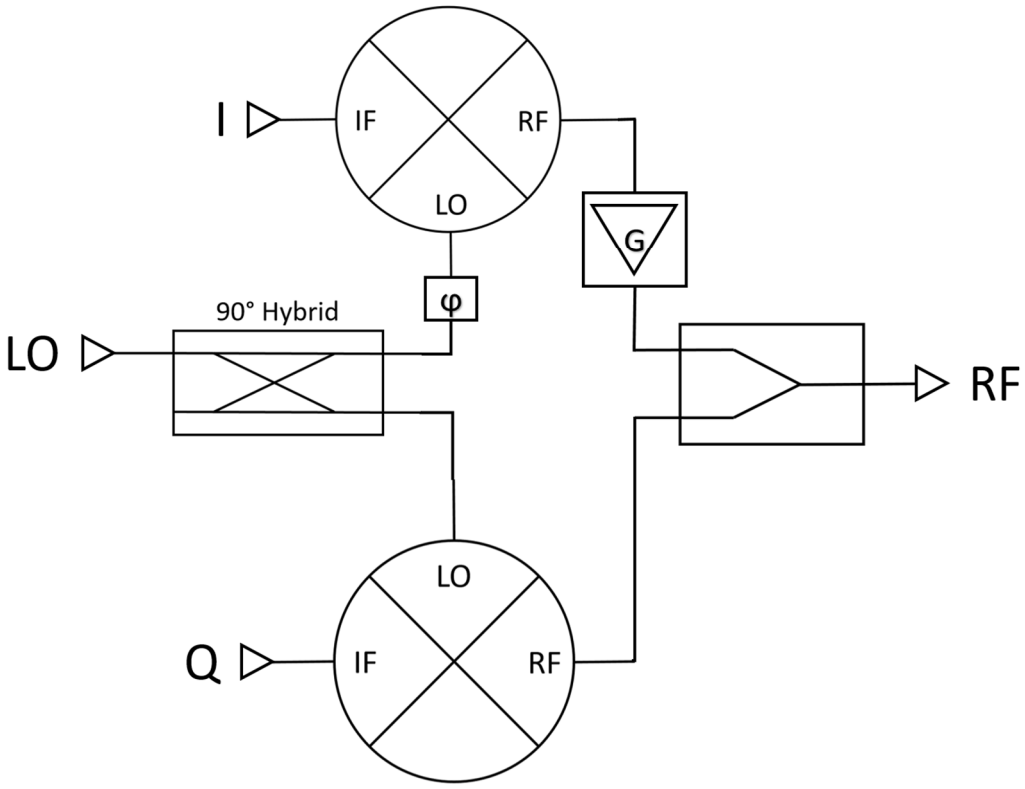

Figure 6: IQ-Mixer with imbalance

2.3.2. Nonlinear Effects

A Mixer fundamentally relies on nonlinear transfer functions of its internal structure. The wanted effect is of course the modulation of the two input signals I and Q with the LO. In a real Mixer the same effect also affects each individual path of the Mixer. Most signals that are fed into a Mixer are arbitrary and contain a wide range of frequencies. The Mixer will modulate these frequencies with each other the same way it modulates the input signal with the LO. This is called intermodulation. This thesis will focus on single sinusoidal input signals so intermodulation won't be a concern. The second, and for this thesis, most important nonlinear effect is called harmonic distortion. If the Taylor series expansion (2) from Chapter 2.1 is not stopped at the second order, (16) shows that even a single sinusoidal input into a nonlinear system will cause it to produce multiple outputs. The output signal will contain multiple sinusoidal components with the frequency of those components being integer multiples of the original input signal frequency. For an IQ-Mixer this effect takes place in both input paths independent from each other [11]. The output or RF path will also introduce harmonic distortions but those are at too high frequencies to be measured.

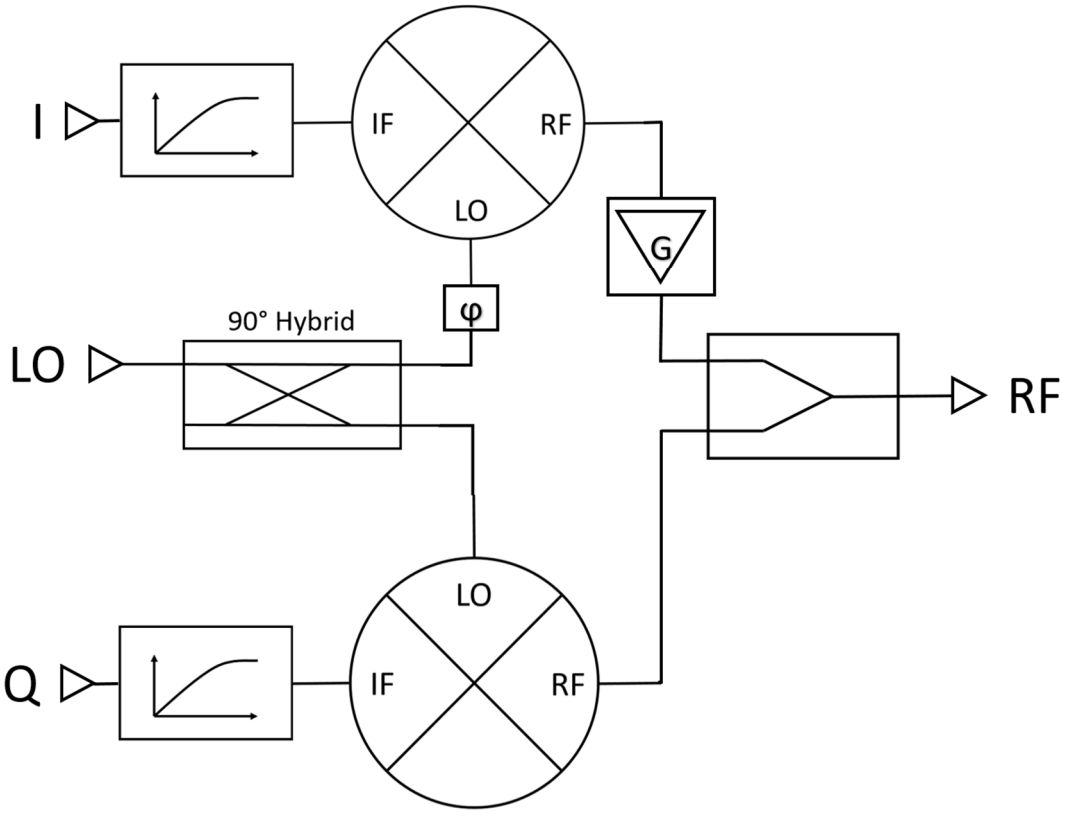

Figure 7: IQ-Mixer with imbalance and nonlinearities

$$e^x \approx x + \frac{x^2}{2} + \frac{x^3}{6} + \frac{x^4}{24} + \cdots + \frac{x^n}{\mathrm{n!}} \qquad (16)$$

2.4. Predistortion

To improve the performance of the Mixer a technique called predistortion will be used. The idea is to characterize all the non-ideal properties of the Mixer. With this knowledge, it is possible to predict the output of the Mixer including all the unwanted signals. To improve the output those unwanted signals are then fed into the input of the Mixer on purpose. If the amplitudes of those signals are exactly the same and the phase is changed by 180° the unwanted signals generated from the Mixer will interfere destructively with the additional signals on the input and cancel each other out. A graphical explanation is shown below. In Figure 8 the device under test is directly fed with a signal and produces unwanted harmonic distortions. In Figure 9 the input signal is first fed through a predistortion unit. It will produce the same unwanted harmonic distortions as the DUT itself but with an additional 180° shift in phase. This predistorted signal is then fed into the DUT and the harmonic distortions will cancel out. The improvements are limited by how accurate the system can be characterized and how precise the signals can be generated. Another limiting factor is that each of those predistortion signal components will again be the source of intermodulation and harmonics itself and taint the result.

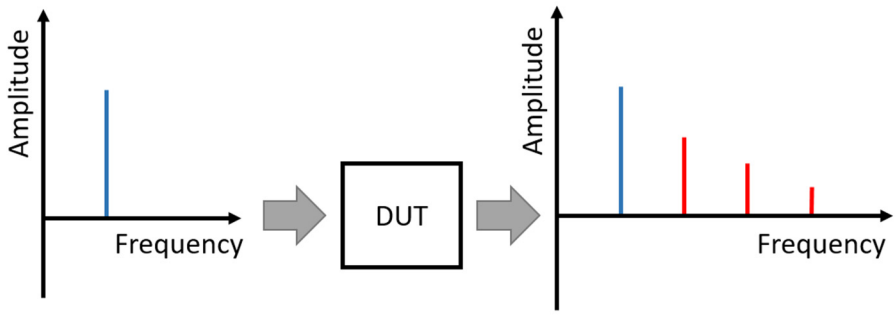

Figure 8: DUT producing unwanted harmonic distortions

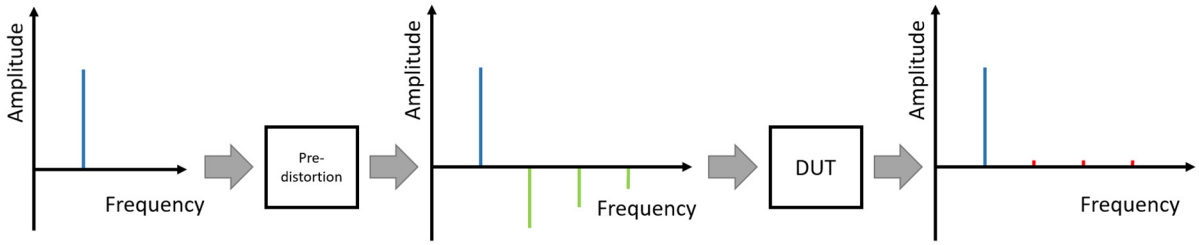

Figure 9: Simple explanation of predistortion

2.5. Physics of Radar systems

Let's start by looking at a very simple block diagram of a pulsed Radar.

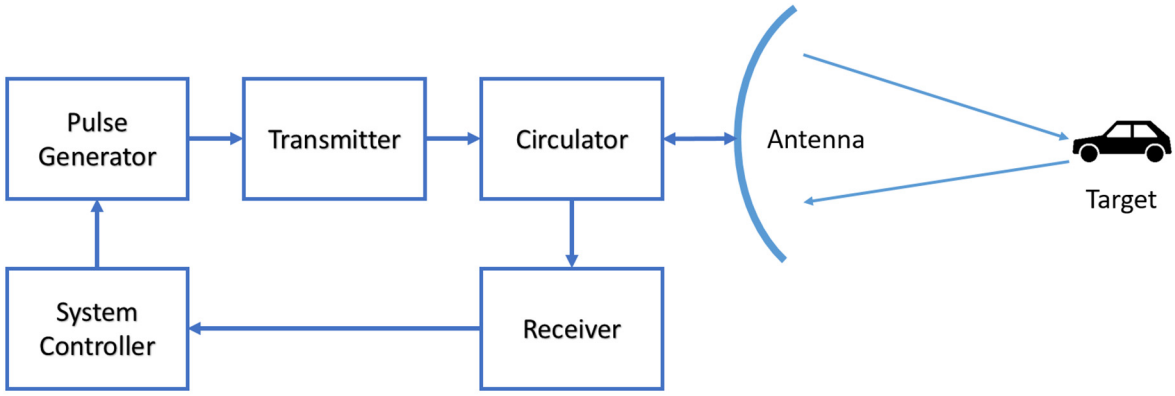

Figure 10: Simple block diagram of a pulsed Radar system

The pulse generator produces very short pulses at a given carrier frequency. A commonly used frequency in automotive Radars is 77 GHz. The transmitter amplifies this signal and then it will be sent out with the help of an antenna. Pulse generator and amplifier are often combined into one device that can generate high power, high frequency pulses all at once. The circulator is a passive component that ensures that the signal from the transmitter is directed to the antenna and not to the receiver. The information received by the antenna will be redirected to the receiver. This allows the Radar to use only one antenna for transmitting and receiving. After the signal is send out by the antenna a target like a car will reflect a part of that signal back to the Radar. The receiver amplifies everything that is picked up by the antenna and listens for those reflections. The system controller knows exactly when a pulse was send out and with the time difference to the received echo it can calculate the distance to the target [12].

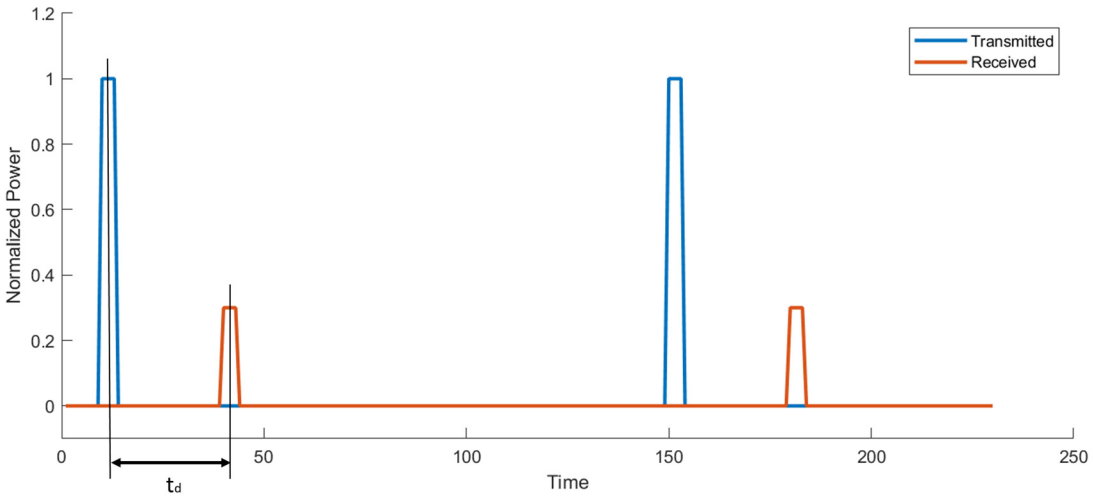

Figure 11: Transmitted pulse and received time delayed echo

$$t_d = \frac{d}{c} \tag{17}$$

$t_d \ldots Delay$
$d \ldots Distance\ to\ target$
$c \ldots Speed\ of\ light$

If the target was moving the frequency of the received signal will also be shifted according to the Doppler Effect. This shift in frequency can be used to calculate the relative speed between the Radar and the target.

$$f_D = 2 * f_0 * \frac{v_T}{c} \tag{18}$$

$f_D \ldots Doppler\ frequency$
$f_0 \ldots Transmit\ carrier\ frequency$
$v_T \ldots Target\ velocity$
$c \ \ldots Speed\ of\ light$

Since the antenna of the Radar system stays constant, the amplitude of the received signal is mainly influenced by the distance and the reflectivity of the target. Since we already know the distance, we can used the receive signal's amplitude as an indicator of the size and reflectivity of the target.

$$P_r = \frac{P_t * G_t * A_r * \sigma}{(4\pi)^2 * R^4} \tag{19}$$

$P_r \ldots Received\ Power$
$P_t \ldots Transmitted\ Power$
$G_t \ldots Antenna\ Gain\ of\ Transmitter$
$A_r \ldots Effective\ Area\ of\ receiving\ Antenna$
$\sigma \ \ldots Radar\ Cross\ Section\ (RCS)$
$R \ \ldots Distance\ between\ Radar\ and\ Target$

2.6. FMCW Radar

One of the drawbacks of a pulse Radar is that all the energy of the signal is confined within a very short pulse. This means that very high power levels are needed for those pulses and all the components must be able to handle these power levels. One way of reducing the peak power is to use another type of Radar. A **F**requency **M**odulated **C**ontinuous **W**ave Radar does not use single pulses but transmits a signal with constant power and varies (modulates) the frequency of the signal. [13]

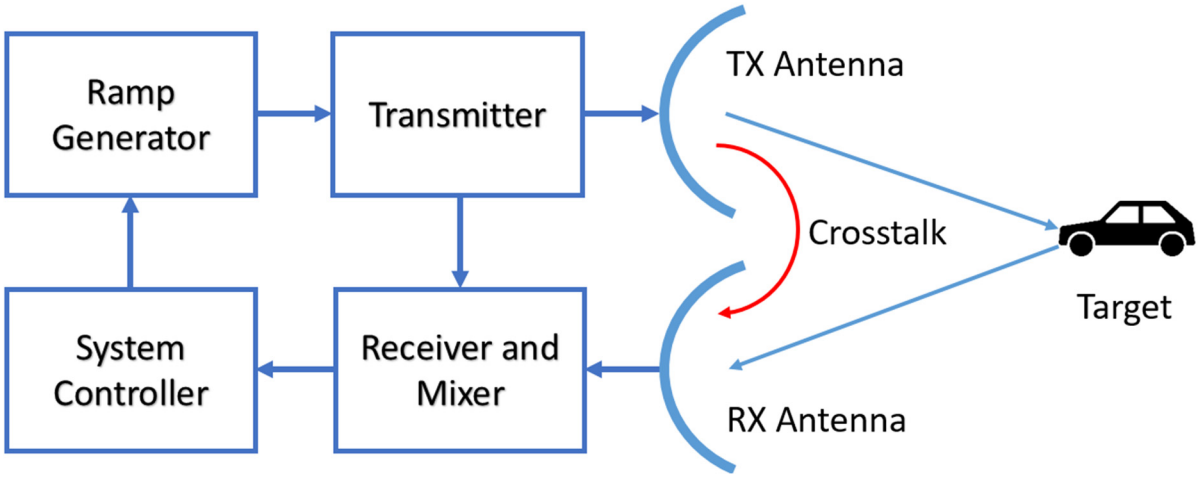

Figure 12: Block diagram of a FMCW Radar

The most commonly used form of modulation is a simple ramp, at which the frequency increases linearly over time. The ramp is defined with a start frequency, a stop frequency, the time it takes to sweep from start to finish and the time between one ramp and the next one. This allows the Radar to transmit the same energy over a longer time period with much lower power. To get the target distance, it is no longer sufficient to measure the time between transmitted and received signal because the signal is transmitted way longer than the echo needs to come back. If the frequency of both signals is plotted over time it will look similar to Figure 13. The distance to the target is now, like the Doppler shift, also a frequency shift of the received echo. The further the distance to the target, the longer the signal needs to travel back. This means the difference in frequency, which is called beat frequency, also gets higher.

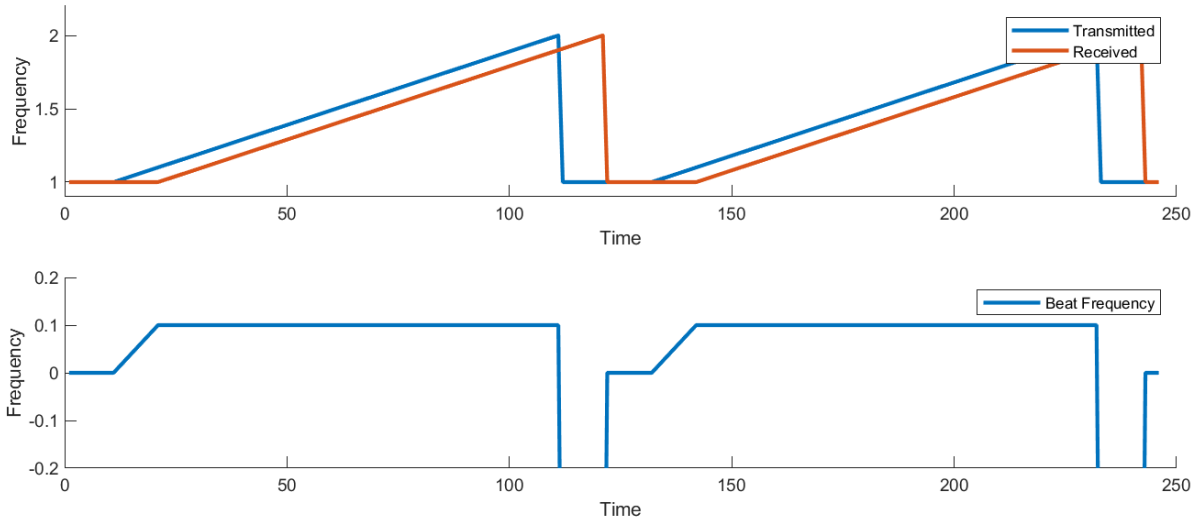

Figure 13: FMCW Radar transmitted and received signal

Since both signals are usually in the GHz-range it would be very challenging to measure this small difference in frequency. To make everything a lot easier the received signal is converted down with a Mixer using the transmitted signal as local oscillator. What a Mixer is and what it does was already explained. The results of this operation (ignoring the summation of booth signals which is about double the transmitted frequency and very easy to filter) is exactly the wanted beat frequency. The IF output of the Mixer is then fed into an analogue to digital converter and further digitally processed. The start and end of each ramp may provide misleading estimation results and are simply ignored in post processing. To get the speed or Doppler shift of a target in this scenario it is necessary to transmit more than one ramp. The distance to the target will always result in the same beat frequency but the Doppler shift will change the starting phase of each new received ramp. Since the signal is now transmitted and received at the same time it is necessary to achieve a high isolation between the transmit branch and the receive branch of the Radar. Using two different antennas for this purpose is an appropriate way to achieve this goal. Any remaining crosstalk causes a small part of the transmitted signal to be received immediately without any delay and, therefore, without any shift in frequency. This results in a beat frequency of zero or a DC offset after the Mixer. The DC offset corresponds to zero distance and is ignored in post processing. If it gets to large, it will cause same part of the signal chain to go into compression and block the wanted signals. For this reason it is simply called the Blocker and must stay below a certain threshold.

2.7. Range Doppler Map

A very powerful way of visualizing the data from a Radar is called a Range Doppler Map. It is a 3D plot capable of showing multiple targets at different distances and speeds. It is calculated with multiple fast Fourier transformations (FFT). The FFT converts the time domain signal into the frequency domain which makes it easy to show one or more discrete frequencies in the IF signal. As discussed previously an ideal single target will result in a single beat frequency on the IF signal. This would give a single peak somewhere on the distance/frequency axis if the target does not show a Doppler shift. The beat frequency is either displayed as a frequency in Hz or it is converted into a distance in meter to show the distance of the target directly. A Doppler shift moves the peak away from the centre v=0 line of the plot. The Doppler shift is measured by recording multiple FMCW ramps. The number of ramps dictates the resolution of this measurement. If 256 ramps were used, the FFT will also have 256 results. These results are called bins and are often directly displayed. With the knowledge of the precise settings of the Radar these bins can also be converted into a relative velocity between the Radar and the target [14].

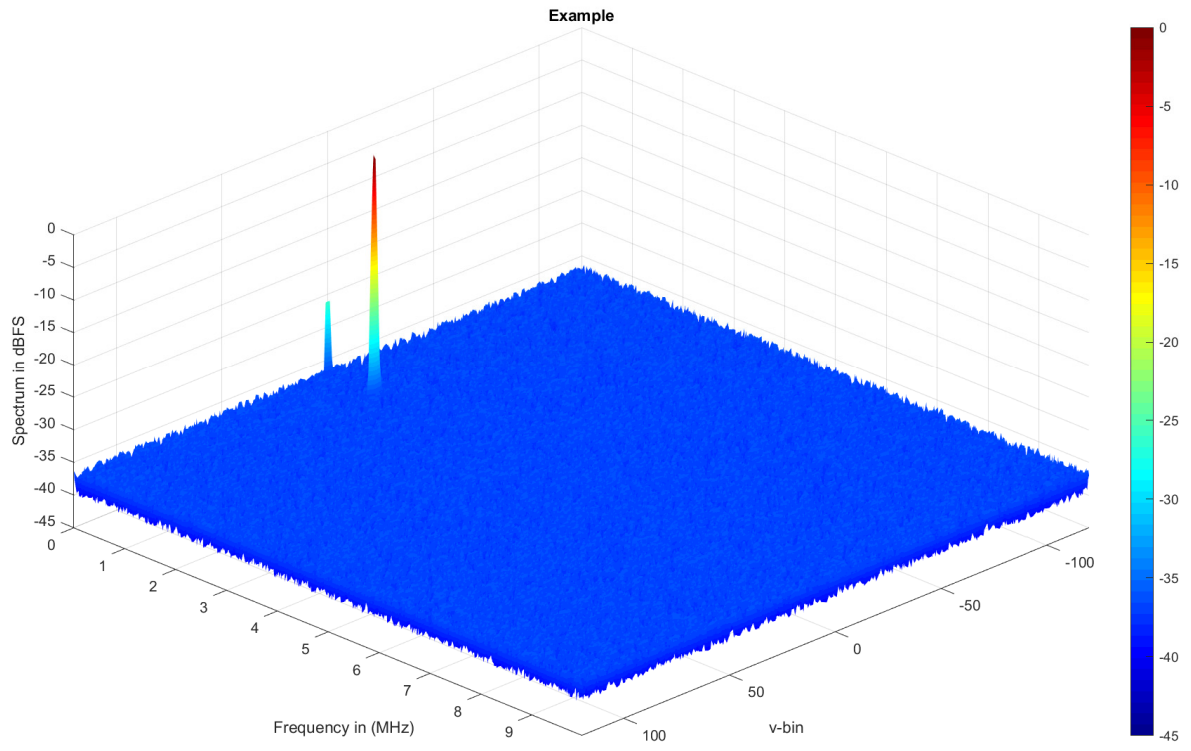

Figure 14: Example Range Doppler Map

The most important factors are the level, position and shape of the main peak. The surrounding noise floor can also give a lot of information on unwanted signals. At the example presented in Figure 14, the noise floor is clean and the main peak is very sharp at 1 MHz in the zero-velocity bin. If the system would introduce additional harmonics those would be visible as additional peaks also in velocity bin zero but at multiples of 1 MHz if the noise floor is low enough. Figure 15 shows an example with harmonic distortions visible up to the 5th harmonic. They are all at a different power level but still have zero Doppler shift applied to them and their frequency is an integer multiple of the main peak. The last visible important component

not yet described is the peak at zero frequency. This part is caused by direct crosstalk between the TX and RX antenna with a very small distance between the antennas. This results in a beat frequency that is very low and it is often called the Blocker. The Blocker can be ignored for most applications unless it gets too high in power. In this case it can bring internal amplifier stages into clipping and block the wanted signals of interest.

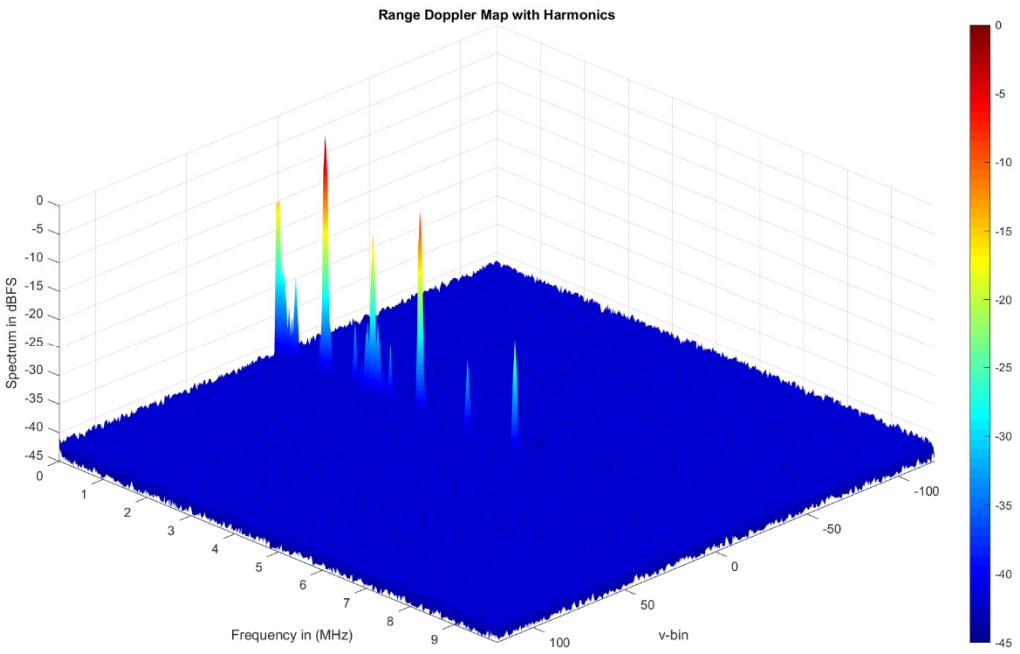

Figure 15: Example Range Doppler Map with Harmonics

3. Experiment

3.1. Goal

The goal of this thesis originates in the wish to replace a very expensive Radar Target Stimulator with a cheaper IQ-Mixer to test available automotive FMCW Radar systems. To do this the transmitted signal from the Radar needs to be shifted down in frequency. This downshift will show up one-to-one as beat frequency in the Radars intermediate frequency (IF) path and will then be displayed as a single target on the Range Doppler Map. The most important part was that only one peak will show up in the final Range Doppler Map. To achieve this a number of experiments or measurements were performed with the IQ-Mixer.

3.2. Experiments

The first experiment in Chapter 4.3 ignored all frequency changing effects of the IQ-Mixer and focuses only on the leakage of the LO signal from the Radar to the output of the Mixer. This signal is responsible for the so-called Blocker and should be as low as possible (see Chapter 2.6). To reduce this LO leakage a DC voltage is applied to the I- and Q-inputs of the Mixer. This changes the internal bias points of the Mixer and directly effects how much of the unchanged LO signal leaks through to the output of the Mixer. During those measurements a very high dependency on the temperature of the Mixer was discovered and tested.

The next step in Chapter 4.4 was to characterize and compensate the linear errors of the Mixer described in Chapter 2.3.1. It also describes a fast way to measure a lot of data points at once to speed up the whole measurement.

Chapter 4.5 tries to characterize the harmonic distortions described in Chapter 2.3.2 and compensate those with a model-based approach. Even though the simulations looked very promising with this approach, the measurements didn't agree. Most probably because the basic model of a diode was too simple for the IQ-Mixer.

After the failure with the model, a machine learning platform was able to find a good solution. This is described in Chapter 4.6.

With the knowledge of all the previous steps it was possible to place the IQ-Mixer in a setup with a Radar sensor and trick the radar into seeing a single target.

4. Measurement

4.1. Devices under Test

For the first measurements to characterize the IQ-Mixer a device from QuinStar Technologies was used. After the DC experiments to improve the LO leakage another Mixer with a better LO suppression was used. Chapter 4.3 explains in more detail why this decision was made. Beginning with Chapter 4.4 a “SFQ-60390315-1212SF-E1-M” from Eravant (formerly Sage millimetre) was used [15]. The Mixer is inside a small metal enclosure (see Figure 16). The I- and O-inputs can be connected to SMA cables and operate in a frequency range from DC to a couple GHz. The LO input and the RF output are located on the remaining two side of the enclosure. Those two connections carry signals in the frequency range of 76 GHz to 81 GHz and are therefore implemented as WR12 waveguides. Additionally, the Mixer needs +5V for internal biasing connected on the dedicated bias input. Unless noted otherwise the Mixer was always at room temperature.

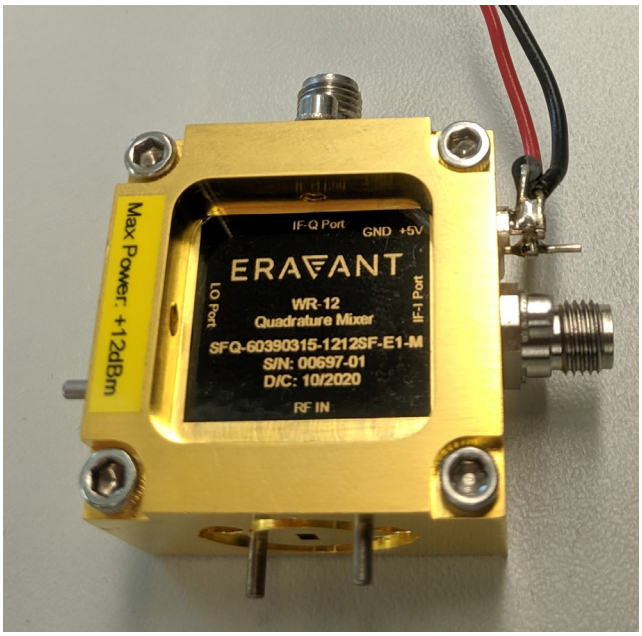

Figure 16: Device under test, Eravant IQ-Mixer

4.2. Measurement setup

To characterize the Mixer the measurement setup in Figure 17 was used. To keep the schematic simple the +5V supply of the x3 multiplier and the +5V bias of the Mixer were omitted. Both were supplied by the same benchtop power supply from two different channels.

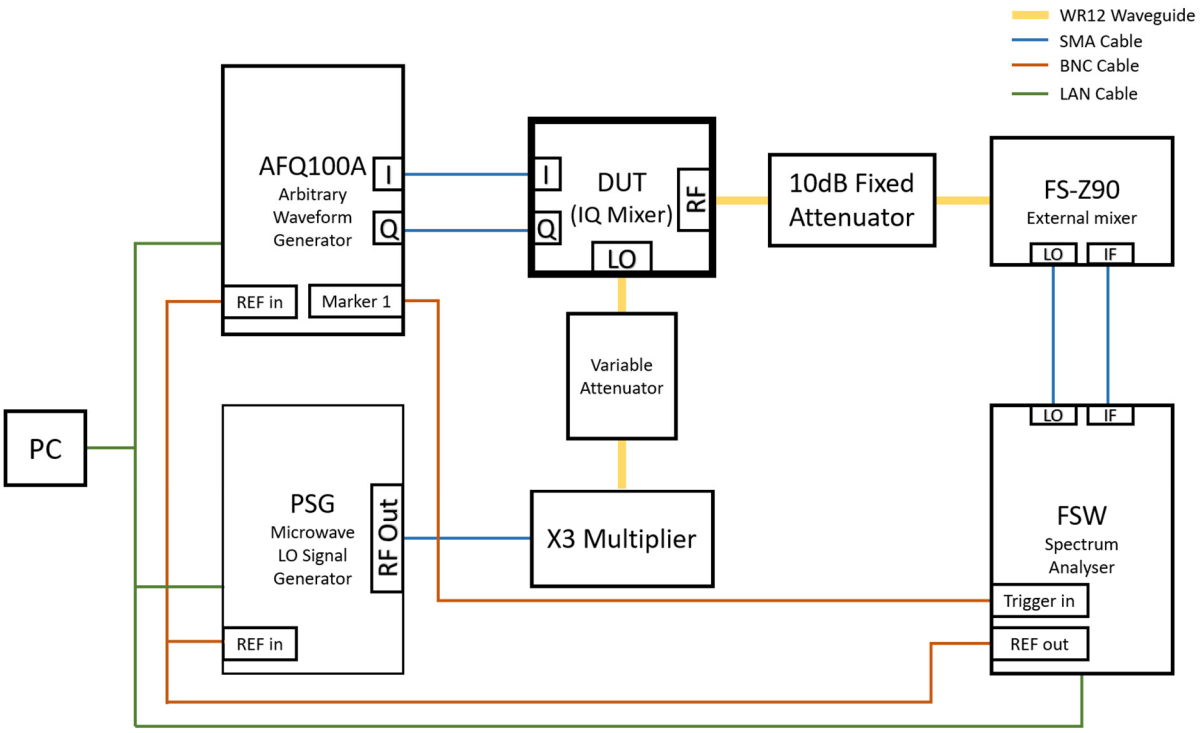

Figure 17: Block diagram of measurement setup

To start with a controlled setup the LO signal for the Mixer was provided by an external generator instead of the Radar. To get a signal with the desired frequency a generator with an attached x3 active multiplier was used. The multiplier triples the frequency of the generator and also amplifies the signal to provide enough amplitude for the LO of the Mixer. This configuration allows good control over the frequency and is mechanically easier to build than a generator that can directly provide the necessary high frequency and power. The output power of the multiplier is fixed and a bit too high for the Mixer. Therefore, a variable attenuator was placed between the multiplier and the IQ-Mixer. To set the power of the LO, a power meter was first connected instead of the Mixer. Using the power meter, the attenuator was adjusted until the power was +8dBm at 78GHz.

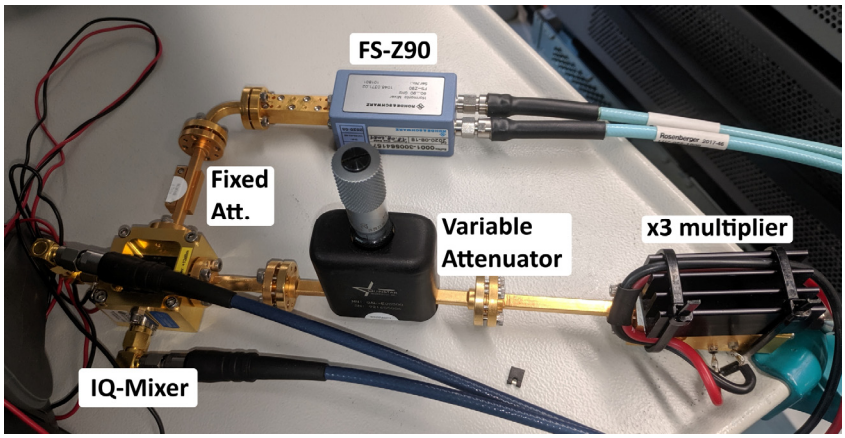

Figure 18: Photo of the Mixer part of the measurement setup

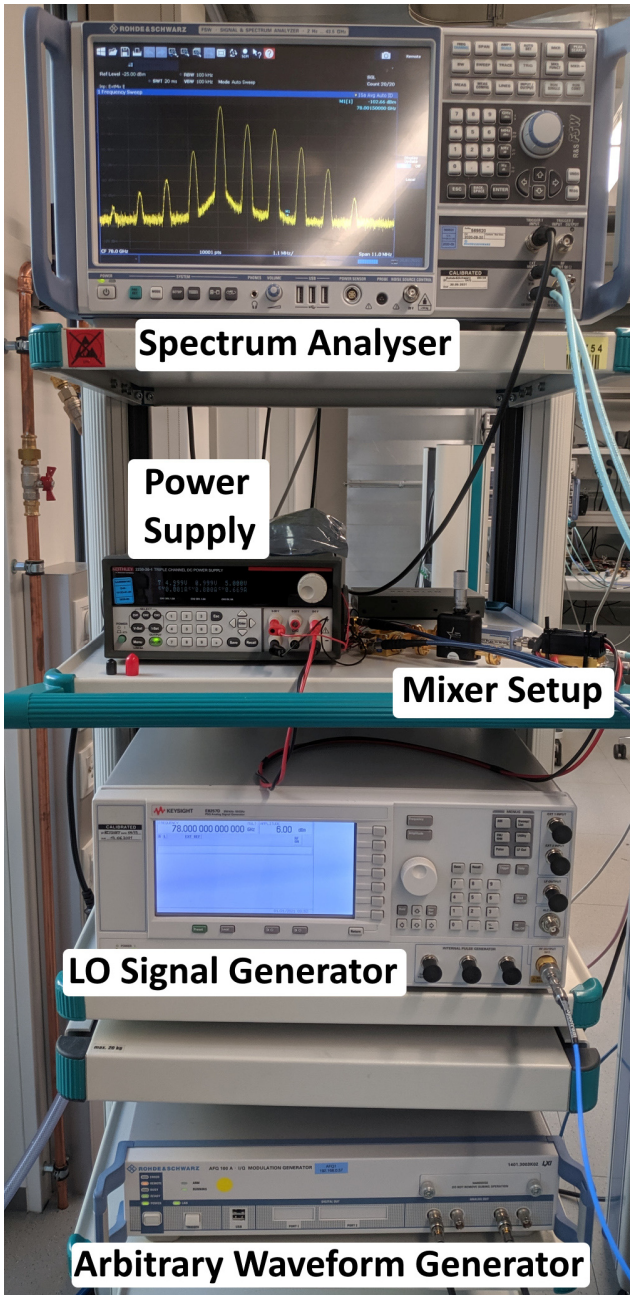

Figure 19: Photo of the measurement setup

The microwave signal generator is a 40 GHz Keysight E8257D better known as a PSG. It is often referred to as one of the best microwave signal generators available on the market and provides a very clean and accurate source for the LO of the Mixer. The I- and Q-input signals are created digitally with MatLab. A Rohde and Schwarz AFQ100A is used as a very good digital to analogue converter and can directly produce the IF input signal for the IQ-Mixer providing a sufficient high fidelity. It is capable of delivering an arbitrary signal with up to 400M Samples/s with 14 bits of resolution. The required input signals are generated with well over 60dBs dynamic range. The output of the IQ-Mixer is connected to a fixed 10dB attenuator. This attenuator provides a safety margin to not damage the harmonic Mixer FS-Z90. This Mixer is applied to extend the operation frequency range of the spectrum analyser. The mentioned attenuator also forces an acceptable level of matching between the IQ-Mixer and the FS-Z90. In this way a decoupling of these two nonlinear devices is achieved, avoiding the creating of spurious emission caused by the measurement setup only. The FS-Z90 provides a WR12 waveguide input to be compatible with the rest of the system and can operate on frequencies between 60 GHz and 90 GHz. It uses an external LO signal that is provided by the spectrum analyser to convert the high frequency on the input to a much lower frequency on the IF port. Using this approach the analyser only needs to be capable of handling the much lower IF frequency and provide a LO to the Mixer. It also makes the setup much easier to build because the LO and IF to the spectrum analyser are flexible SMA cables instead of rigid waveguides. The spectrum analyser is a FSW from Rohde and Schwarz which is one of the most capable spectrum analysers on the market. All those devices are linked together with a 10 MHz reference signal. All internal and generated frequencies in this setup are derived from this 10 MHz reference. Otherwise, each device would use its own frequency reference. The small difference of the different reference oscillators is already sufficient to generate frequency offsets in the same size as the one we want to measure. With the 10 MHz link a 78 GHz signal generated by the signal generator + multiplier is also measured as exactly 78 GHz on the spectrum analyser. One additional link is from a Marker output on the AFQ to the trigger input on the spectrum analyser. This is not strictly necessary but was used to speed up the measurement process.

Using this measurement setup three important parameters of the IQ-Mixer behaviour were characterized: the LO leakage, the gain and phase imbalance as well as the nonlinear distortion products present at the Mixer's output. Using these characterization result I can use the same measurement setup to apply predistortion techniques for compensating the undesired part of the Mixer response.

4.3. LO Leakage

The first Mixer from QuinStar had a very high LO leakage. This leakage can be reduced by adjusting the bias of the Mixer with a DC voltage applied to the IQ inputs. The manufacturer recommends to stay below 300mV on both inputs to not damage the device. For this task a slightly modified version of the schematic shown above was used:

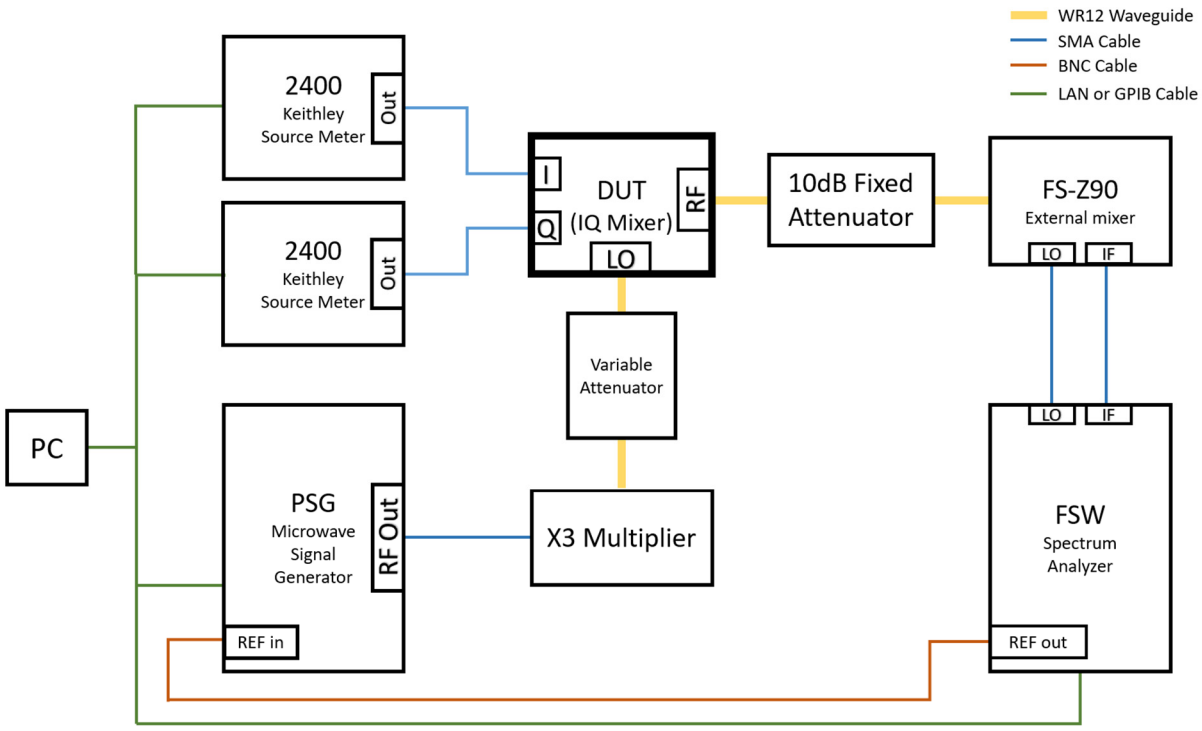

Figure 20: Block diagram for DC optimization measurement setup

The only difference is the two Keithley source meter units which were used instead of the two outputs of the AFQ. A source meter unit can provide a very accurate DC voltage and has a much higher dynamic range compared to the AFQ. They can also measure the current flowing into the device with very high accuracy. To get a better LO rejection the Mixer needs a very precise bias voltage applied to both inputs. To find this voltage a 2D search was performed by sweeping the DC voltage from 0V to the 200mV on both channels and measuring the LO level for each point. At every sweep 11 different output voltages per Source Meter were set resulting in 121 measurements in total. After each sweep the voltages associated for the minimum in LO leakage were used as starting point to calculate the next sweep. Hence, every successive sweep the minimum LO voltages of the last sweep defined the new midpoint of the next sweep. At the same time, the step size for the sweep was decreased by a factor of 10. With this method it was possible to find the maximum LO rejection within a couple of minutes and push the LO leakage into the noise of the spectrum analyser. These measurements were repeated for a bunch of different LO frequencies as the LO leakage shows a frequency dependent behaviour. Figure 21 highlights the level of the LO rejection relative to the uncompensated Mixer performance over the considered frequency span of 75 GHz – 81 GHz.

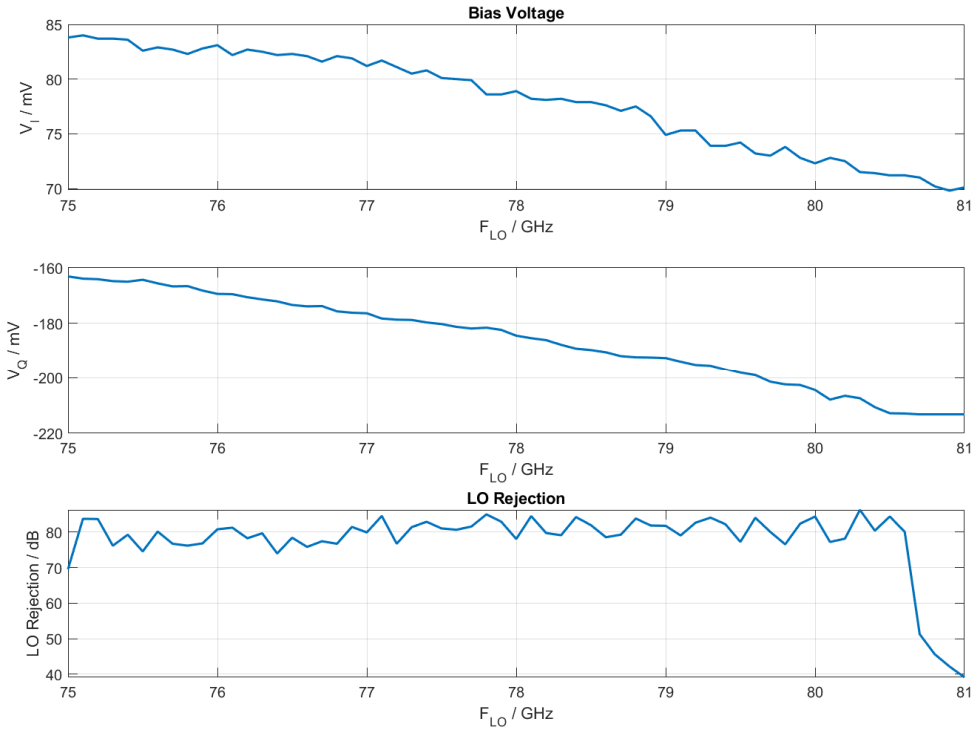

Figure 21: Results of DC optimization

The relationship between the applied DC-voltages and the associated LO rejection is summarized by the 3D graph shown in Figure 22.

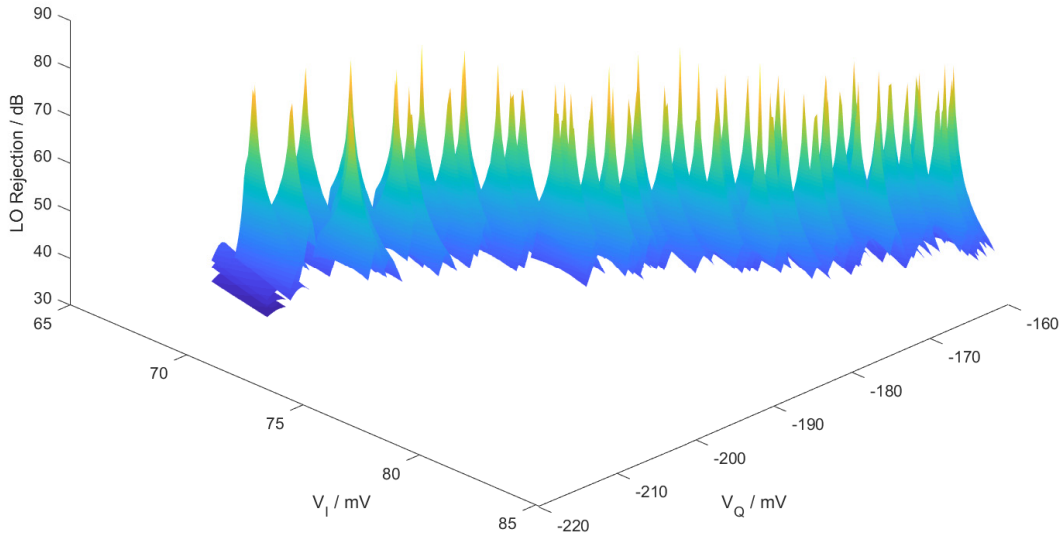

Figure 22: 3D representation of DC optimization with 0.1mV steps

It is easy to see that the DC voltage needs to be very precise to achieve the desired LO rejection of better than 70 dB. During the measurements another unwanted effect was discovered: The LO leakage of this device is very sensitive to the ambient temperature. At my laboratory environment I recognized a temperature fluctuation of about 1-2 °C. This was already enough to increase the LO leakage again by more than 20 dB as shown by the figure below

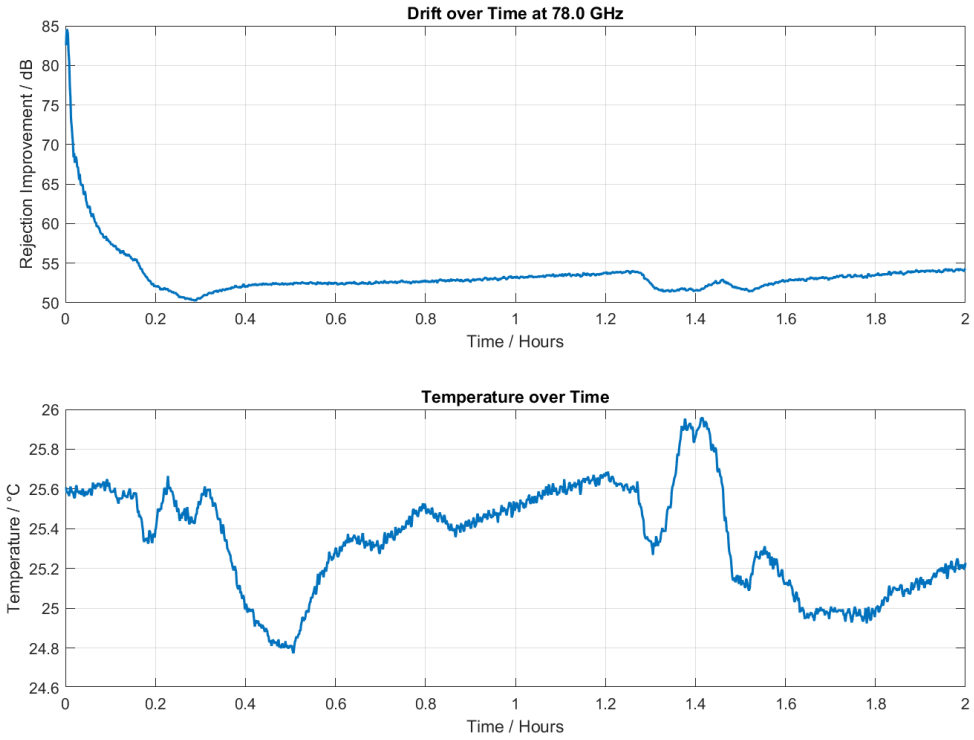

Figure 23: LO rejection degradation over a short time

As indicated in Figure 23, within 10 minutes the LO leakage increased again by more than 30 dB despite of a very stable temperature. At this measurement, the temperature probe touched the metal housing of the Mixer providing a good thermal contact. The measurement equipment and the Mixer were warmed up for more than 30 minutes before the measurements started. A very clear dependency on the temperature can be seen in Figure 24. This measurement that was taken over a weekend with nobody in the Lab. An attempt to use a Thermostream (a temperature forcing device using compressed air to keep a DUT at a specified temperature) did not yield any improvements on this topic either.

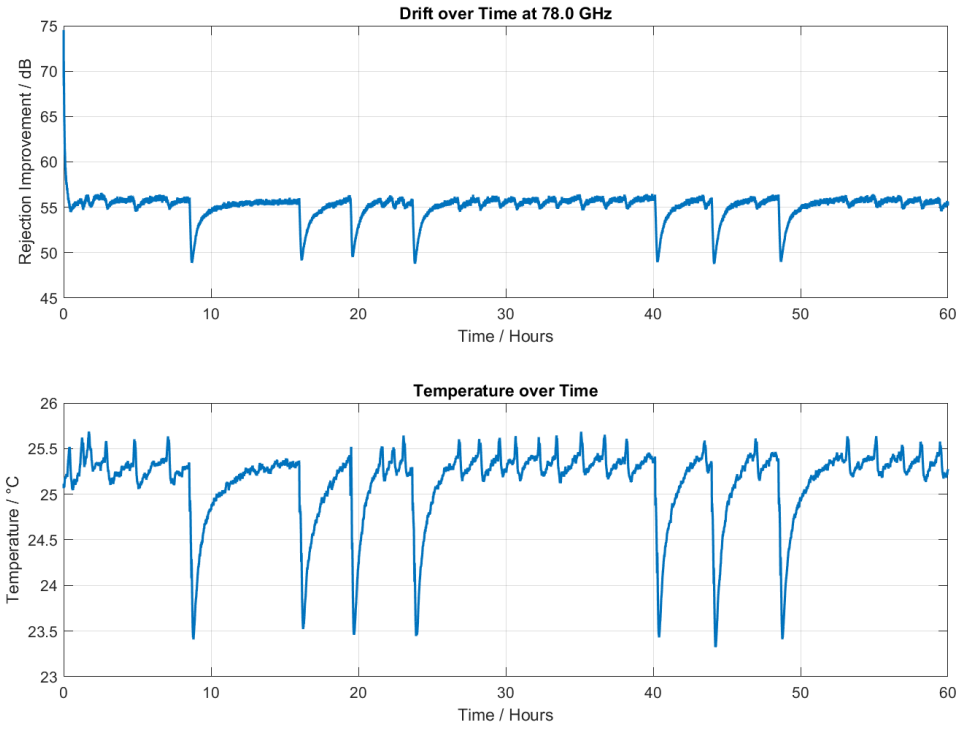

Figure 24: LO rejection degradation over a weekend with temperature influence

In Figure 24, dips in temperature of about 2°C are observable. These dips were caused by a very powerful air conditioning system with a rather stupid thermostat to control it. To permanently achieve a stable LO leakage rejection of better 70 dB a very precise temperature controlled and thermally isolated environment would be required. This specification is probably even higher than commercially available temperature-controlled solutions.

Even though the rejection drifts away from the desired performance it is still a lot better than without any DC bias adjustments and would be enough to be useful for the desired application. The biggest drawback of this method is the needed DC level. It is very high in comparison to the maximum allowed level and would limit the amplitude of any future signal too much. It also brings the Mixer in a very nonlinear operating point which makes its usage even more difficult and unpredictable. For those two reasons, I decided to continue to work without any DC voltage and use a Mixer with a better LO suppression.

4.4. Gain and Phase Imbalance

Due to the LO leakage problem at the QuinStar Technology Mixer summarized in the last section, the investigation of the gain and phase imbalance compensation was continued using the Mixer from Eravant. The manufacturer advised me to not apply any DC voltage to the IF inputs. Since it showed a much better LO leakage suppression out of the box it was no longer necessary. The goal of this step was to find the value for the phase and gain correction to get a high-performance single sideband modulation. To define a baseline for this task, a sinewave of f = 1 MHz with an amplitude of A = 100mV was chosen as the IF input signal. I applied the same signal at both IF channels. Only an additional phase shift of -90° was introduced at the Q-input to enforce lower sideband output only. At the baseline measurement, the factor G was set to 1 and φ to 0 in this formula:

$$V_I = A * G * \sin\left(2\pi f + (\varphi - 90) * \frac{\pi}{180}\right) \quad (20)$$

$$V_Q = A * \sin(2\pi f) \quad (21)$$

$$V_I, V_Q \ldots Baseband\ IQ\ input\ signals$$

$$A \ldots Peak\ amplitude$$

$$f \ldots IF\ signal\ frequency$$

$$G \ldots Gain\ correction$$

$$\varphi \ldots Phase\ correction$$

The baseline measurements were conducted using a LO level of 8 dBm. Using these settings, the Mixer did not show the expected performance as presented in Figure 25.

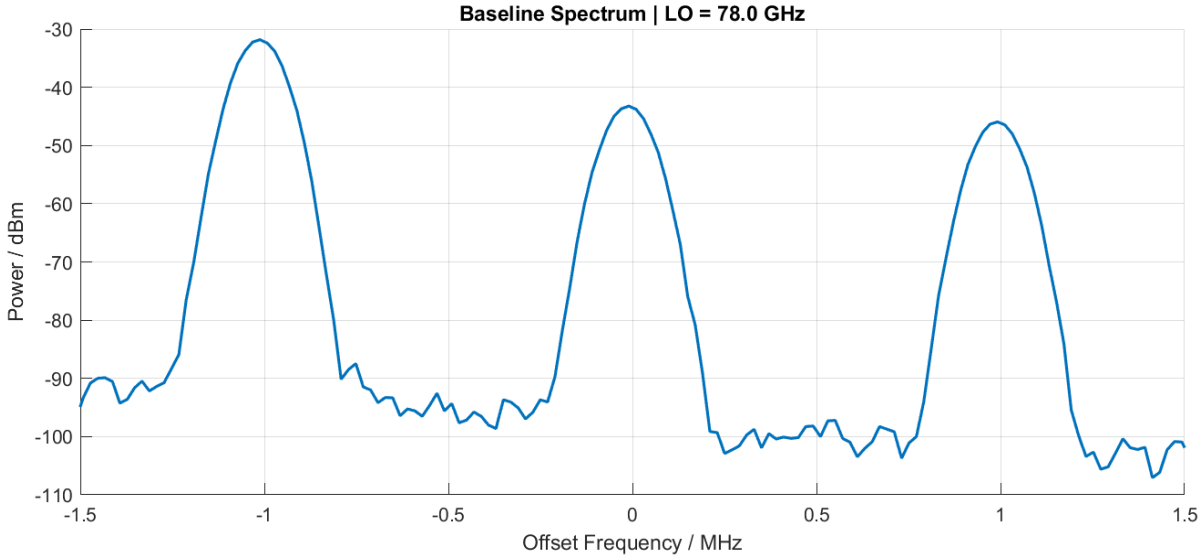

Figure 25: Baseline sideband spectrum without any corrections

The goal for the imbalance compensation measurement campaign was to lower the level of the unwanted sideband to be close to the spectrum analysers' noise level. In this context I use the unwanted upper sideband suppression defined as the difference between the power of the wanted sideband minus the power of the unwanted sideband. The baseline measurement showed a suppression of roughly 15 dB which is insufficient for the desired application. To get a better sideband rejection the two unknown correction factors G and φ must be optimized. Similar to the DC part this was achieved by sweeping both parameters at the same time using an iterative optimization approach.

The Mixer input signals were calculated in MatLab and send to the AFQ via an Ethernet connection. The speed of the process gets slower the longer the signal gets as more digital samples need to be transmitted from the PC to the waveform generator. In a first step, the IF input signals were calculated using one value for G and φ, sending it to the generator and then measuring the result with the spectrum analyser. As this approach required a high amount of data sent between the instruments, it was too slow and would take too long for an efficient implementation. For this reason, the spectrum analyser was set to operate in the zero-span mode. In this mode, it acts as a power detector for one given frequency and plots the power of this frequency over time. In MatLab a special signal was constructed with a whole sweep of G and φ parameters built into one long output signal and sent to the AFQ. Each pair of G and φ was used to generate the corresponding input signal which drove the Mixer for a length of only 10µs. All those 10µs pieces were then simply concatenated together to form one long signal that was then send to the waveform generator. It now drove the Mixer with a signal that changes its properties every 10µs. Additionally, a digital output pulse of the AFQ was generated using one of its marker signals. Every time the signal has played once and started again the marker was toggled. This marker pulse was fed into the trigger input of the spectrum analyser to initiate the start of a zero-span measurement. The zero-span measurement was set to the exact same length as the signal from the AFQ. Back in MatLab this zero span recording is split up again and matched with the G and φ parameters used to generate the IF signals. In this way, the measurement of one G and φ parameter set was reduced to 10µs including a bit of overhead, which was much faster than the initial approach. The drawback of this method is that only single frequencies of the spectrum can be monitored at one measurement and the measurement needs to be redone for every signal in the spectrum. For this measurement campaign, the only interesting signals are the two sidebands. To get a more stable measurement, a lower noise floor was achieved by applying 10 times averaging at the spectrum analyser. The biggest pitfall of this measurement is the resolution bandwidth of this device. This is usually the most crucial parameter. Lowering the resolution bandwidth also lowers the noise floor of the instrument but increases its measurement duration. With that in mind the resolution bandwidth must be higher than 100 kHz or the discrete steps of the IF signals get lost. For a better understanding of this relationship, Figure 26 plots a simple set of three G and φ parameters composing one IF signal sweep. This gives nine parameter combinations for the sweep.

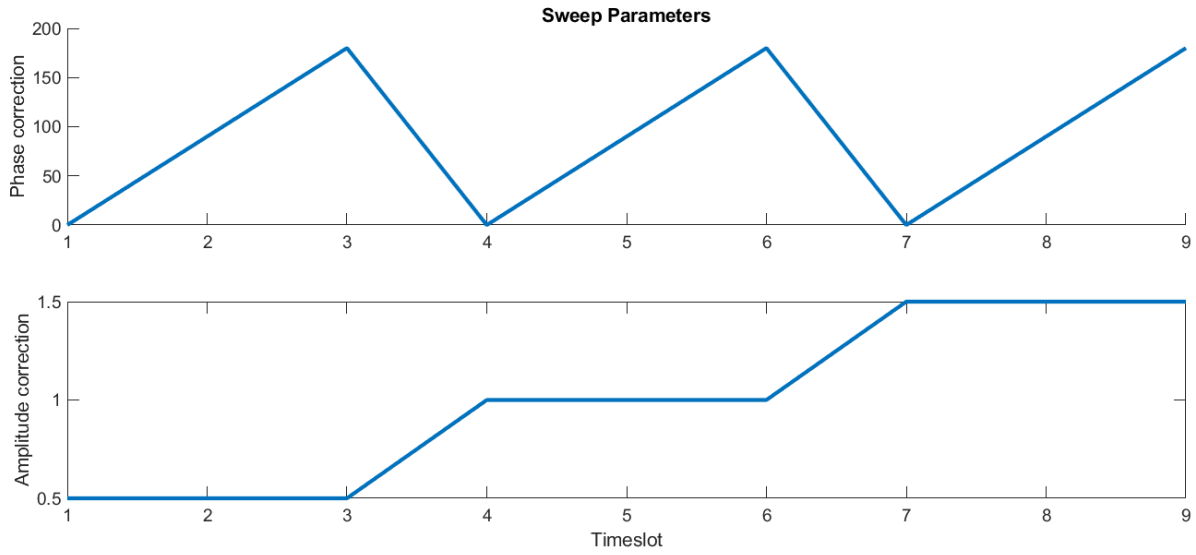

Figure 26: Example of a parameter sweep over time

The resulting IF signals are summarized in Figure 27.

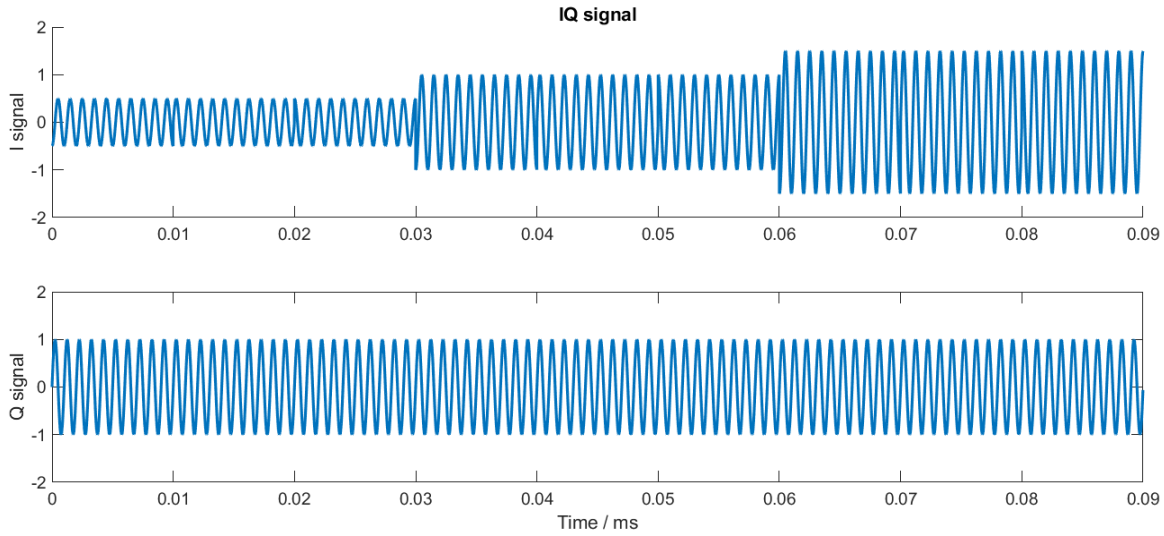

Figure 27: Time domain signal for the example sweep over time

Every 10 µs the IF signals change. The first three times, only the phase changes, then the amplitude changes once and the phase changes for another three times again. This way all nine possible combinations can be measured with one set of signals sent to the AFQ.

A real measurement uses a lot more parameters at once as indicated in Figure 28.

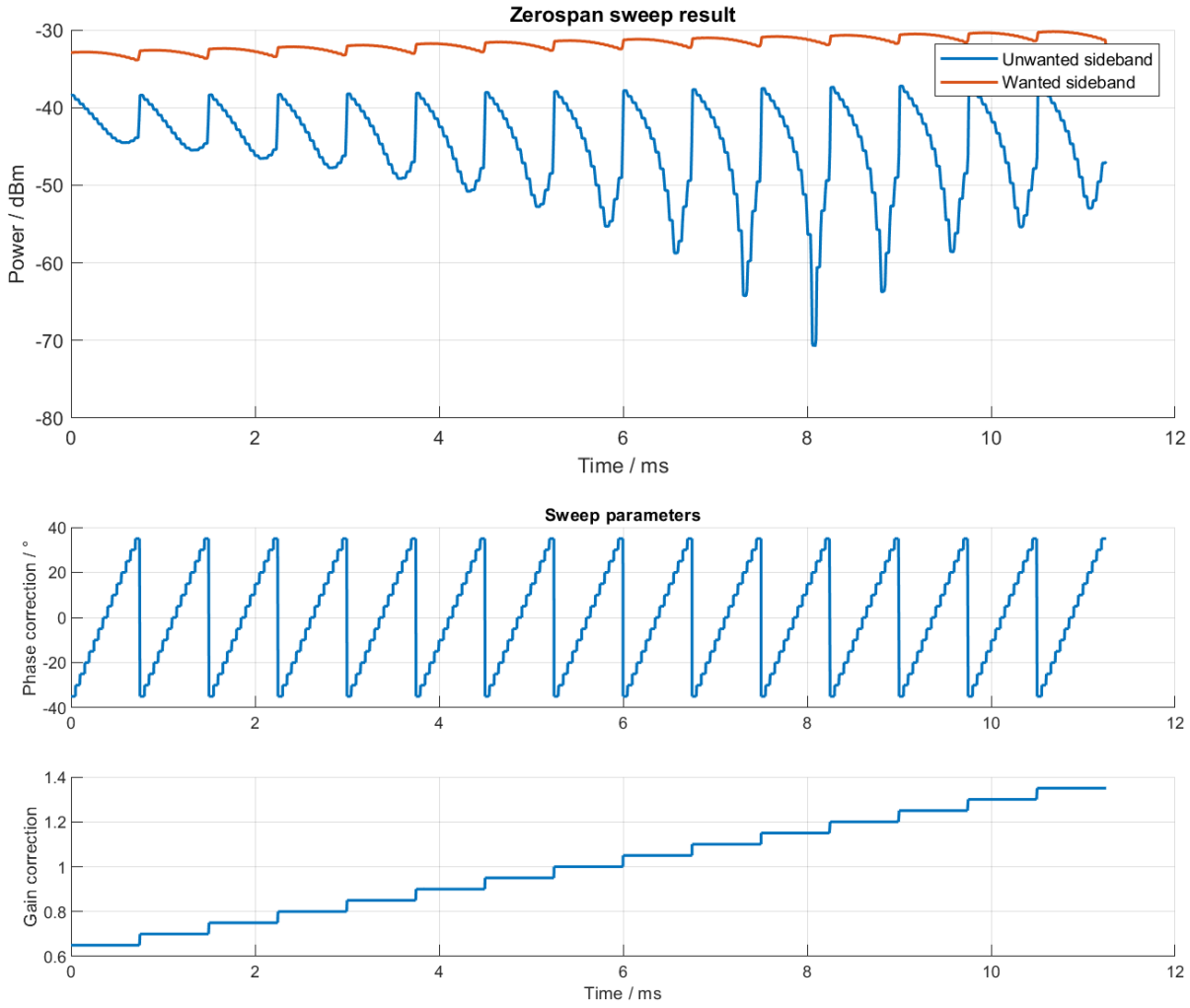

Figure 28: Real zero span measurement and input parameters over time

After each sweep the set of parameters associated with the highest imbalance suppression was derived. These combination of parameters were thereafter used as starting point for the next sweep, applying a finer sweep. This process was repeated until the desired sideband suppression was reached. With this method and equipment a sideband suppression of roughly 60 dB can be reached within about a minute. The spectrum recorded before and after the sideband optimization is presented in Figure 29.

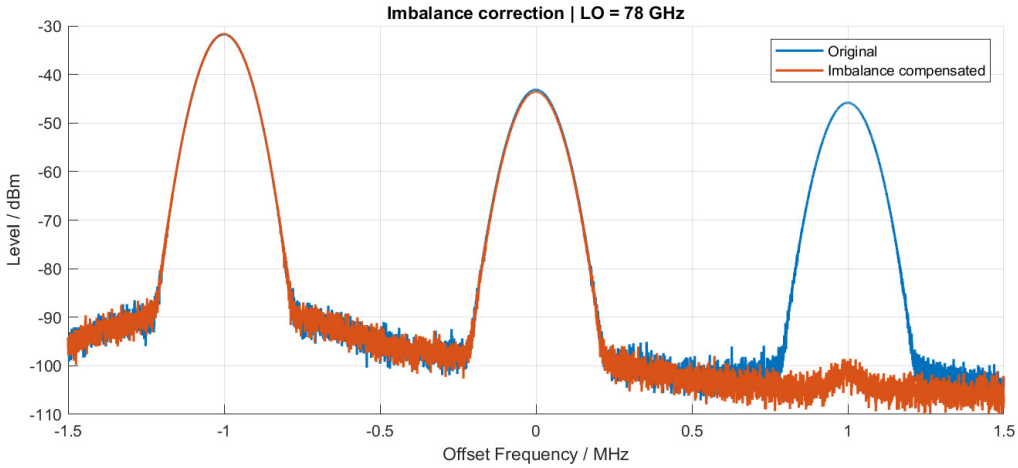

Figure 29: Sideband spectrum after imbalance compensation

Also, the gain and phase imbalance of the Mixer showed a frequency dependent behaviour. Therefore, the imbalance optimization process is repeated for different LO frequencies to get an idea on how the parameters change over frequency. Figure 30 plots the LO frequency dependency of the G and φ parameters recorded in this way. This measurement was also repeated for 3 different IF input frequencies.

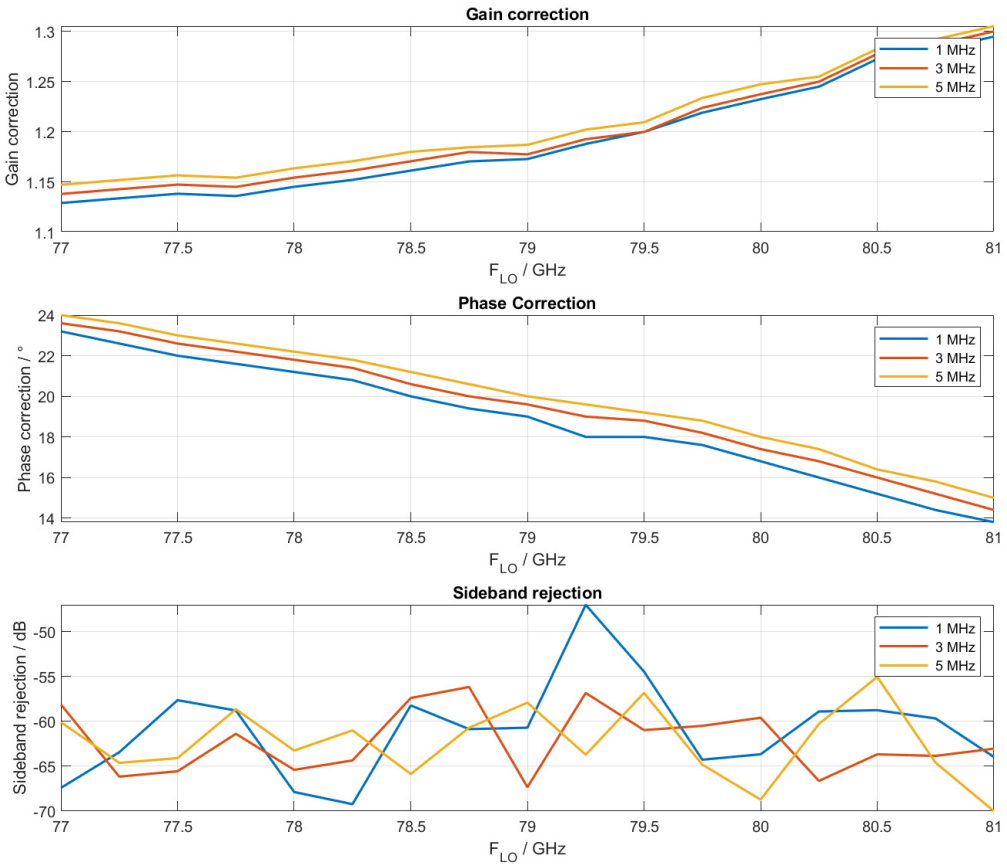

Figure 30: Imbalance coefficients over LO frequency with resulting sideband rejection

Using this information, the linear errors of the Mixer can be compensated for the given LO frequency range, LO input power and IF signal input power.

4.5. Nonlinear predistortion with a model based approach

The spectral plot from the previous results already looks very good but is only part of the truth. If the viewed frequency span on the spectrum analyser is increased a very different picture is seen as indicated in Figure 31.

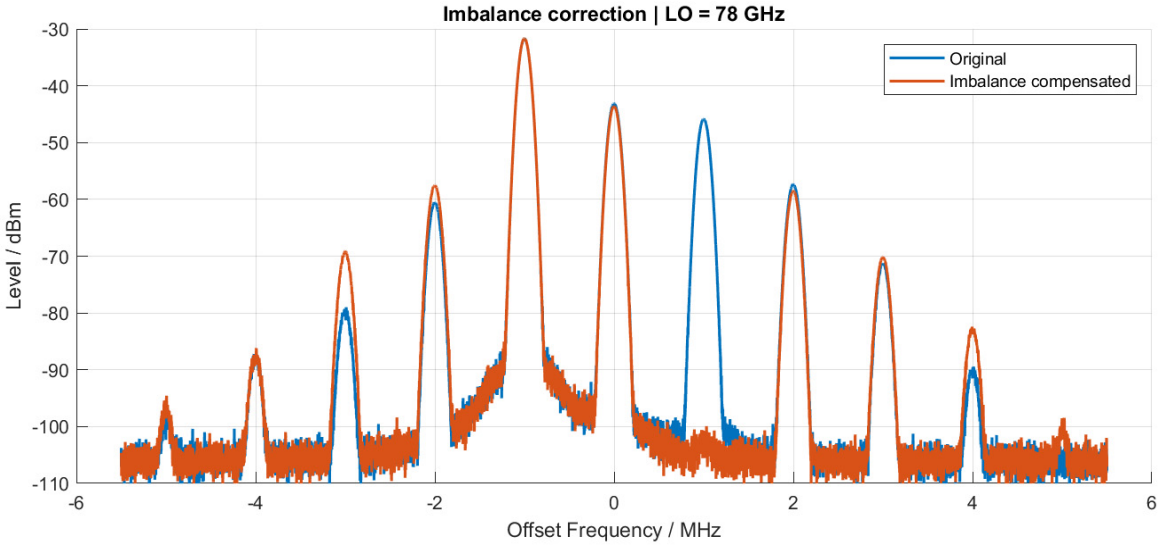

Figure 31: Spectrum after imbalance compensation with multiple harmonics

Compared to Figure 29, no parameters for the imbalance compensation were changed and the unwanted sideband still is the same as before but now the extended frequency range covered by the spectrum analyser sweep highlight the presence of the harmonic distortions created by nonlinear behaviour of the analogue IF section of the Mixer. How those harmonics are created and how to get rid of them was already explained in Chapter 2.3.2 and Chapter 2.4. Harmonic distortions created by the RF part of the Mixer will be at multiples of the LO frequency and are too high to be measured. For this approach a model will be used to describe the harmonic behaviour and calculate the necessary predistortion. According to the simple model of a real Mixer from Chapter 2.3.2, I assume that each input contributes harmonic distortions independent from the other input. Therefore each input will be looked at separately while the second input is set to zero. The chosen model was a simple diode-based model described by (16). It can also be written as a polynomial function like in (22). [16]

$$\mathrm{y} = a_1 x + a_2 x^2 + a_3 x^3 + \cdots + a_n x^n \qquad (22)$$

$$y \ldots resulting\ output\ signal$$

$$x \ldots input\ signal$$

$$a_n \ldots harmonic\ coeffecient$$

$$n \ldots harmonic\ number$$

For this investigation I choose a sinusoidal signal with an amplitude A and a frequency w as input for this nonlinear system:

$$x = A * \sin(wt) \qquad (23)$$

With this input into the nonlinear model the resulting output will be:

$$y = a_1 * A * \sin(wt) + a_2 * A^2 * \sin(wt)^2 + a_3 * A^3 * \sin(wt)^3 \quad (24)$$

Using the product to sum identity for trigonometric functions and grouping them accordingly I derive:

$$y = y_0 + y_1 + y_2 + y_3 \quad (25)$$

$$y_0 = \frac{1}{4} * 2 * a_2 * A^2 \quad (26)$$

$$y_1 = a_1 * A + \frac{3}{4} * a_3 * A^3 * \sin(wt) \quad (27)$$

$$y_2 = \frac{1}{2} * a_2 * A^2 * \cos(2 * wt) \quad (28)$$

$$y_3 = \frac{1}{4} * a_3 * A^3 * \sin(3 * wt) \quad (29)$$

The first part y_0 has no frequency and will be a DC part of the signal. This DC part is generated inside the Mixer and detunes the bias point even if a pure sinusoid signal is applied. The second part y_1 is the wanted signal with the original frequency. It is, however, also impacted by the contribution of the 3rd harmonic since $a_3 \neq 0$. The second (y_2) and third (y_3) harmonic only include their associated coefficients a_2 and a_3. This is because in this calculation only frequencies up to the third harmonic were included at the presented analysis. In reality, also higher order nonlinear products can provide important contributions to this model.

The model presented in (24) is a valid approximation if the Mixers behaviour follows the mentioned diode-based characteristic. Based on this assumption I can calculate a predistortion function compensating this response up to a desired nonlinear order.

I choose again a polynomial function to represent the inverse behaviour of (22) but with different parameters:

$$\mathrm{x}_p = b_1 x + b_2 x^2 + b_3 x^3 + \cdots + b_n x^n \quad (30)$$

$$x_p \ldots predistorted\ input\ signal$$

$$x \ldots original\ input\ signal$$

$$b_n \ldots inverse\ harmonic\ coeffecient$$

$$n \ldots harmonic\ number$$

With the procedure described in [17] the inverse coefficient result to:

$$b_1 = \frac{1}{a_1}$$

$$b_2 = -a_1^{-3} * a_2 \quad (31)$$

$$b_3 = -a_1^{-5} * (2 * a_2^2 - a_1 * a_3)$$

The coefficients a_n must be chosen to represent the behaviour of the Mixer observed in the measurements. In theory it should be sufficient to sweep the amplitude of the input voltage

and the voltage of the output signal should follow the described polynomial curve. MatLab can then be used to conduct a least-square optimization for matching the coefficients to the measured response. The results of this sweep can be seen in the next plot:

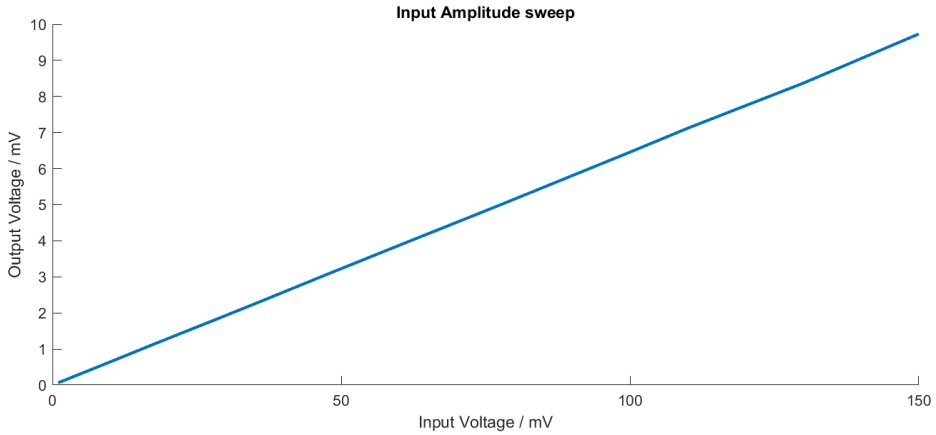

Figure 32: Limited input level sweep

The damage free input power range specified by the Mixer's manufacturer is unfortunately way too low to see a reasonable nonlinear response as shown by the plot in Figure 32.

Another way to get the coefficients is already provided by equation (25) to (29). Every harmonic can be investigated at individually and the coefficients can then be compared to the amplitude predicted by the corresponding relationship. For example, the amplitude of the second harmonic only contains the initial input amplitude A and the coefficient a_2 :

$$2 * a_2 * A^2 * \cos(2 * wt) \qquad (32)$$

The coefficients can be measured with the small exception that the sign of the coefficients can't be measured with the spectrum analyser since it only measures the absolute power of the spectral components. Therefore a positive and negative amplitude show the same result and the measurement will always give a positive coefficient. This is no problem for the simulation and for the real device it can only be plus or minus for each harmonic and is quickly figured out by trying both possibilities. For the I-input of the Mixer using a 100mV input signal the power levels relative to the wanted fundamental signal are:

2. Harmonic	3. Harmonic	4. Harmonic
-20.05 dB	-45.72 dB	-56.60 dB

With those values the polynomial coefficients were calculated and fed into a simulation of the nonlinear model. The simulation only consists of the formula (22) to describe the model of the Mixer and should give the same results as the measurement. For the simulation a time discrete sampled sinusoid is created. Every single sample of this sampled signal is put through formula (22) to simulate the Mixer. To analyse the result a Fast Fourier Transformation (FFT) was used to transform the time domain signal into the frequency domain. This separates the individual parts of the signal by their frequency which then can be compared directly to the measurement results from the spectrum analyser. The simulated results were close to the measurements, at least for the lower harmonics as presented in Figure 33.

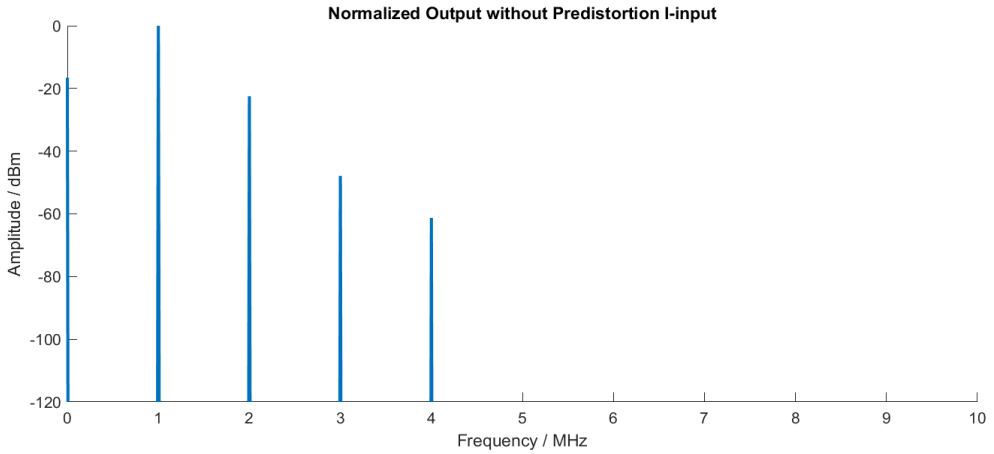

Figure 33: Simulated output spectrum with a model of the Mixer

Using the coefficient modelling the measured Mixer response, the needed parameters for the inverse polynomial are derived using (31). As the predistorted Mixer input signal is intended to compensate the nonlinear distortion of the model, the amplitude of the spectral components generated by the predistortion function and the model are of equal size, as can be seen by comparing Figure 33 and Figure 34. In case of the predistorted response also nonlinear distortion products exceeding the one in Figure 33 are present.

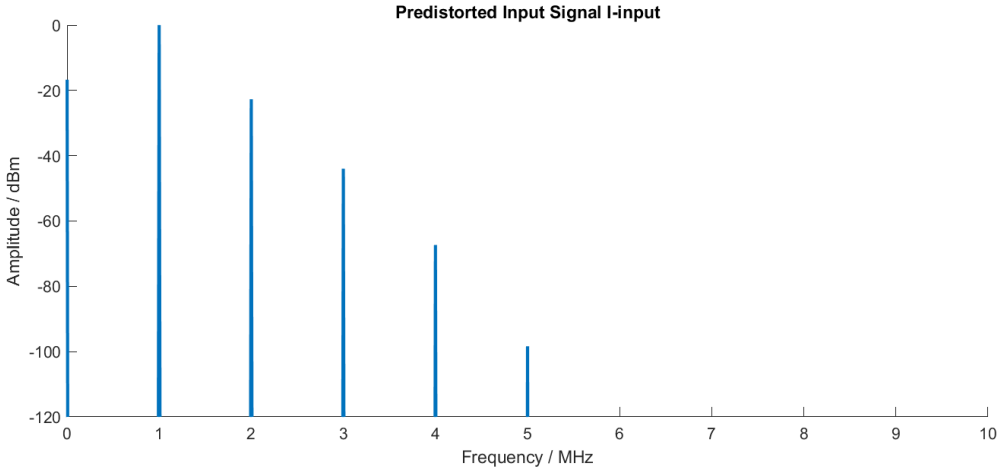

Figure 34: Spectrum of the needed predistorted input signal with the model

This predistorted signal is then used as a new input signal into the Mixer. Simulating this concatenation of the predistotion and the Mixer model shows some very promising improvements as highlighted in Figure 35.

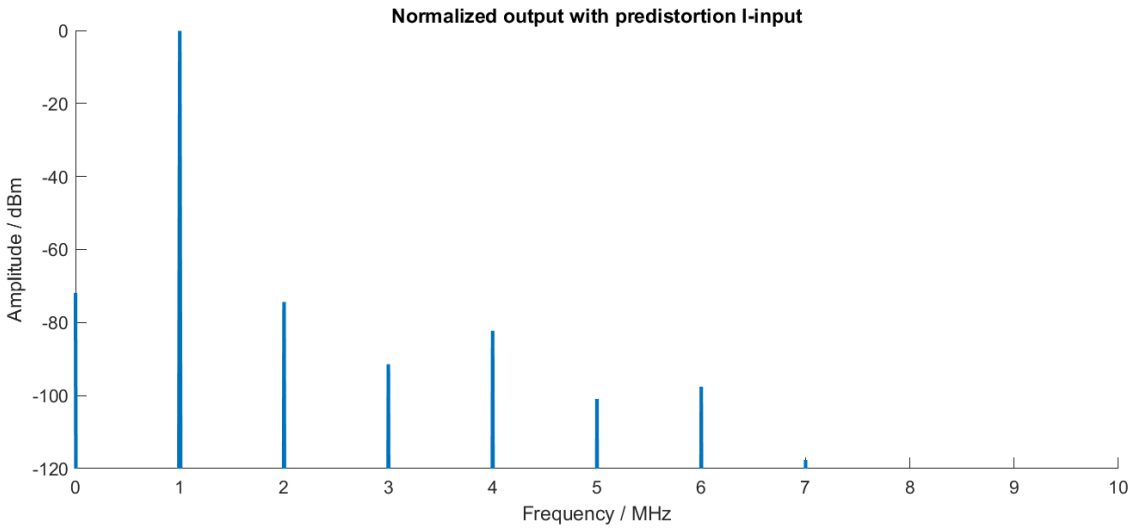

Figure 35: Simulated resulting output spectrum with the predistorted input signal

The harmonic levels improve by at least 50 dB in the simulation. It can also be seen that the predistortion is responsible for creating new even higher harmonics although at a very low level in this arrangement.

For the implementation of this approach using the Mixer hardware, in a first step, only the second harmonic was predistorted by setting all coefficients above b_2 to zero. This should only impact the second harmonic and to a small degree the 4th harmonic response.

The measurement however showed multiple problems. Even when applying the correct sign of the coefficient only very moderate reductions of the level of the second harmonic distortion at the Mixer output were observable. This could be improved by sweeping the coefficient over a wider range around the initial value and search for the highest reduction in the level of the distortion. The second finding was even more problematic. While it was possible to reduce the second harmonic at the same time the third harmonic got worse. Such a behaviour is not described by the Mixer model (22). The model itself is the simplest way of a nonlinear system for such a Mixer. I was able to successfully apply this approach for Mixers operating in the lower GHz frequency range. This findings however showed not just some inaccuracies but a fundamental shortcoming of the model. Without knowledge about the exact internal structure of the IQ-Mixer and a lot of work as well as additional measurements this approach will not provide the desired performance required for my application. To keep the scope of this thesis manageable the model based approach was abandoned at this stage.

4.6. Nonlinear predistortion with machine learning

Since the model-based approach did not work, a modeless method equivalent to the linear gain and phase correction was investigated. Each harmonic for each channel was assigned a gain and a phase coefficient. With those additional parameters the input signal function can be written as:

$$V_I = A * G * \sin\left(2\pi f + (\varphi - 90) * \frac{\pi}{180}\right) + A * g_{I,2} * \sin\left(2 * 2\pi f + \left(\varphi - 90 + \varphi_{I,2}\right) * \frac{\pi}{180}\right) + \cdots A * g_{I,n} * \sin\left(n * 2\pi f + \left(\varphi - 90 + \varphi_{I,n}\right) * \frac{\pi}{180}\right) \quad (33)$$

$$V_Q = A * G * \sin(2\pi f) + A * g_{Q,2} * \sin\left(2 * 2\pi f + \varphi_{Q,2} * \frac{\pi}{180}\right) + \cdots A * g_{Q,n} * \sin\left(n * 2\pi f + \varphi_{Q,n} * \frac{\pi}{180}\right) \quad (34)$$

$$V_I, V_Q \ldots Baseband\ IQ\ input\ signals$$

$$A \ldots Peak\ amplitude$$

$$f \ldots IF\ signal\ frequency$$

$$G \ldots Gain\ correction$$

$$\varphi \ldots Phase\ correction$$

$$g_{I,n} \ldots n.harmonic\ gain\ I\ channel$$

$$g_{Q,n} \ldots n.harmonic\ gain\ Q\ channel$$

$$\varphi_{I,n} \ldots n.harmonic\ phase\ correction\ I\ channel$$

$$\varphi_{Q,n} \ldots n.harmonic\ phase\ correction\ Q\ channel$$

$$n \ldots harmonic\ number$$

Now the new parameters $g_{I,n}$ and $\varphi_{I,n}$ need to be swept until a minimum in all observed nonlinear distortion products is found. The Mixer shows recognizable harmonics up to the 5th order. Hence, I choose so n=5 in (33) and (34). This means that additional 16 input parameters are included for the optimization additionally to the linear correction factors. The linear terms are also likely to change a bit so a total of 18 input parameters have to be considered for finding a minimum over all harmonics. This is no longer possible by just trying a coarse sweep and decreasing the step size a bit with each run.

To solve this optimization problem a proprietary company internal new platform called xHub was used. Within xHub experiments can be created. Each experiment can then run by a

number of different so-called controllers. The controller provides the values for all input parameters and records the results. One controller could do a Monte-Carlo run while another one optimizes something. The results are fed to the controller through a REST API and can come from a simulation or a measurement. In the framework of this thesis, the multi object optimizer controller was used. The instrument control script described in Chapter 4.4 was changed to accept input values from xHub and report the measured response back. The multi object optimizer is a machine learning algorithm based on differential evolution [18]. All the 18 parameter were defined as inputs. The results reported back to xHub were the power levels of each sideband and the harmonic distortion. Overall, a total of 10 values were covered in this way. The controller was then told to optimize all harmonics to a minimum without giving more importance to a specific one. As an additional results the spurious free dynamic range (SFDR) was calculated by subtracting the power level of the wanted sideband with the power level of the highest harmonic distortion. This value was also reported back and xHub was told to maximise this value with a higher weight factor. This ensured that all harmonics would be lowered to the same level. Without this trick a couple a harmonics would always be very good but others would be barely below the set threshold.

After about 200 iterations the optimizer found a solution that satisfied the given thresholds. From this point on, the controller began to look for different solutions and optimized these further. This task only took a couple hours and would not have been possible to do in a realistic timeframe without the machine learning algorithm. The given results in the xHub report looked very promising. Figure 36 shows the 10 best results. The x-axis lists the power levels of all harmonics, the unwanted sideband and the SFDR. The y-axis shows the achieved values for each result and if it is below the given threshold. The threshold for each value was chosen after a couple tries in a way that they can be reached. If those thresholds are set too high or too low the algorithm can get stuck. The important information visible in the graph is that all goals could be reached (are in the green part) and that that there is a solution that reduces all harmonics to the same level (flat orange curve number 2).

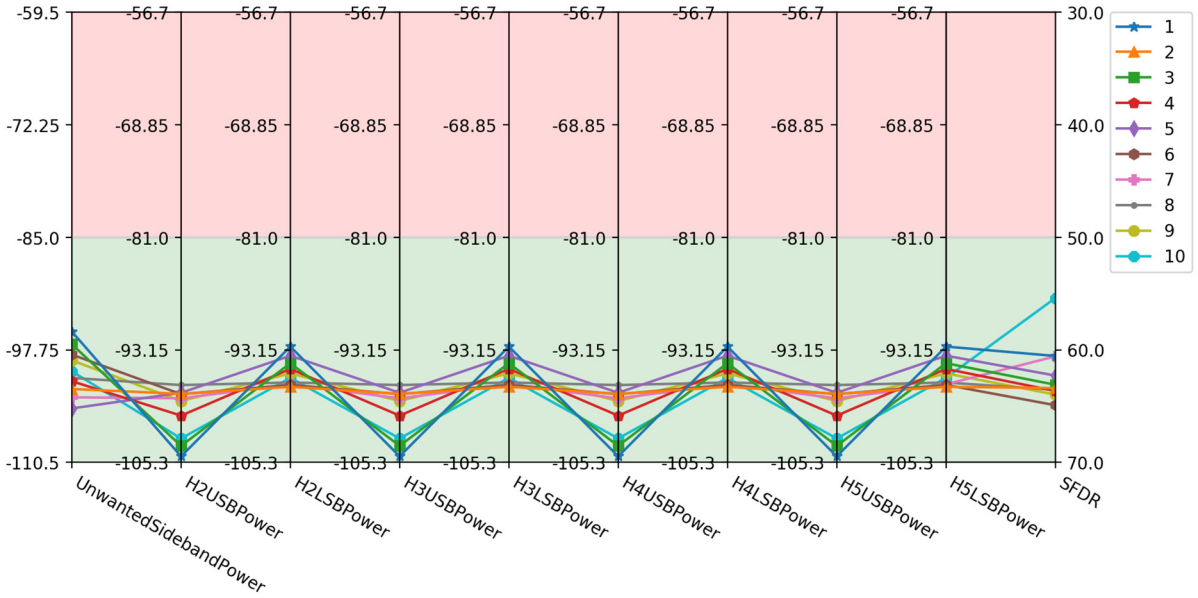

Figure 36: 10 best results from the machine learning algorithm

The result is quite impressive and lowered the highest harmonic to 60 dB below the wanted sideband signal and improved the spurious free dynamic range by over 45 dB. Looking at the spectrum analyser confirms the indicated performance as presented in Figure 37.

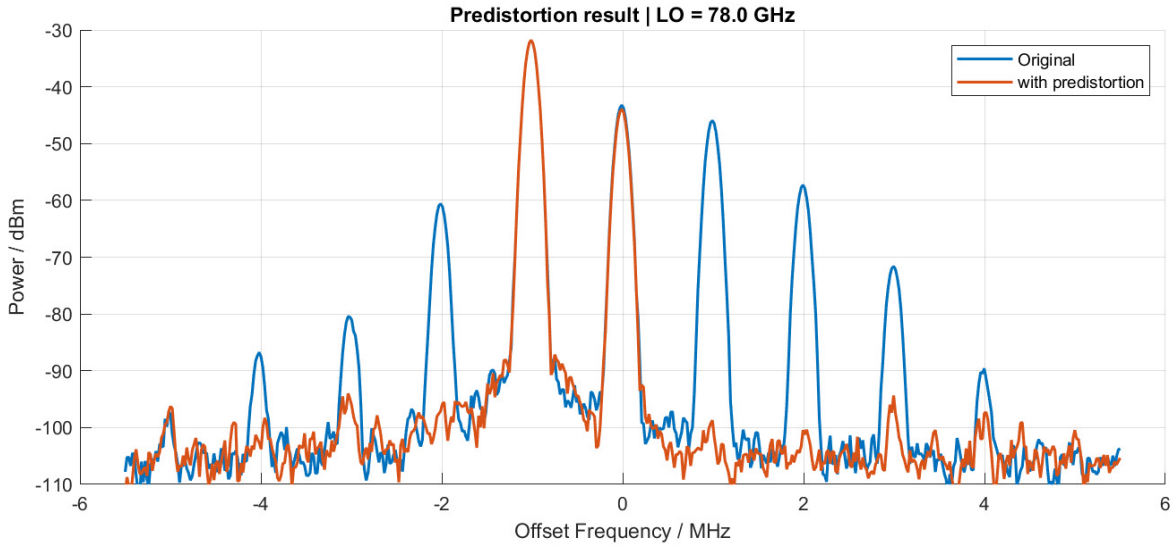

Figure 37: Spectral improvement after nonlinear predistortion

This step is now repeated for different LO frequencies to get a good idea about how the parameters change over frequency.

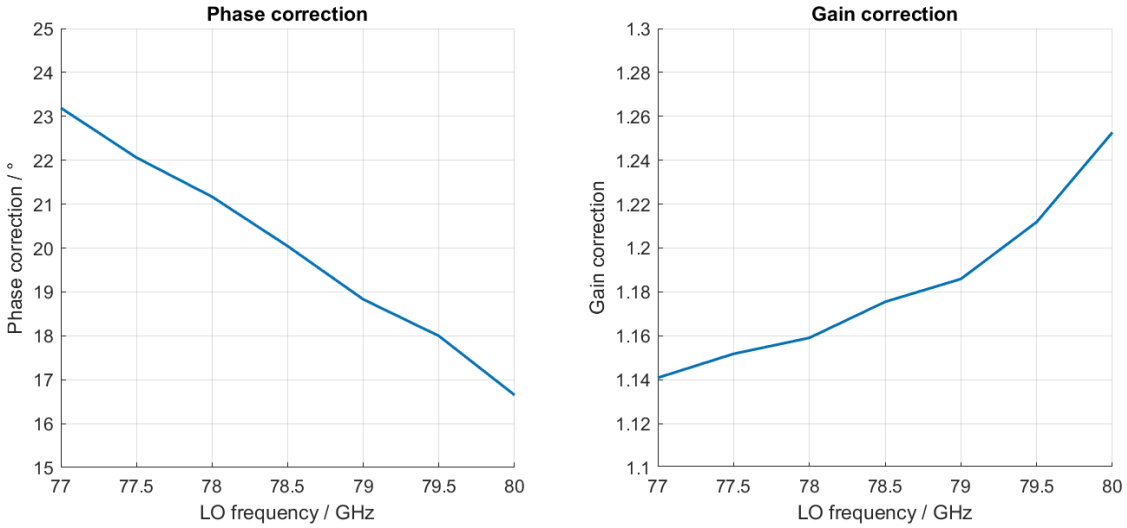

Figure 38: Imbalance parameters over LO frequency for nonlinear predistortion

In comparison to Figure 30, the needed phase correction stays the same but the gain correction shows a slightly different progression. The addition of the harmonic components to the input of the Mixer increased the overall signal amplitude and shifted the Mixer's point of operation. Another contribution comes from the harmonic signals itself. Every odd order harmonic directly adds a bit of strength to the fundamental signal amplitude as shown previously:

$$\ldots + (4 * a_1 * A + 3 * a_3 * A^3) * \sin(wt) + \cdots \qquad (35)$$

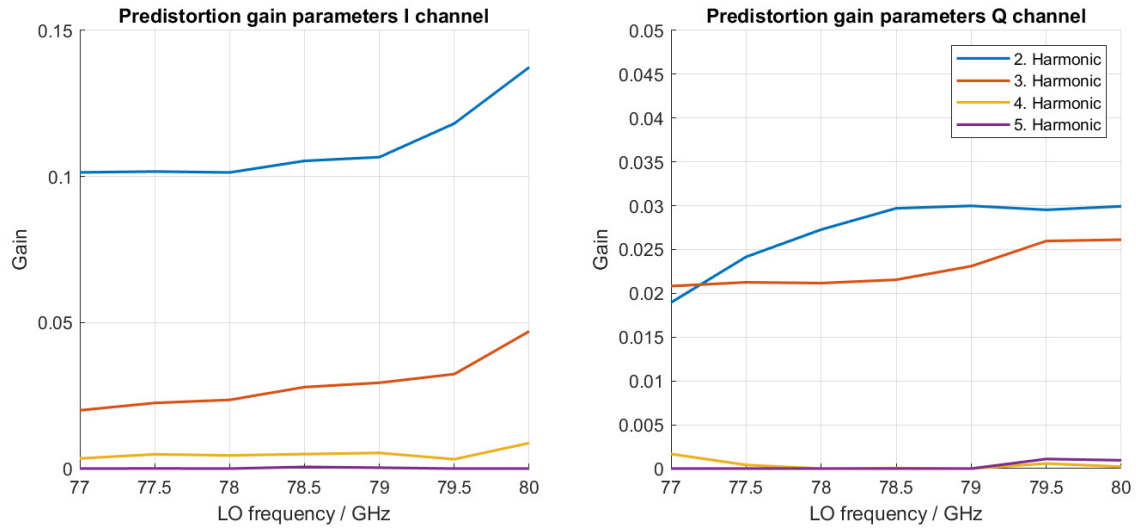

Figure 39: Gain for nonlinear predistortion for each harmonic over LO frequency

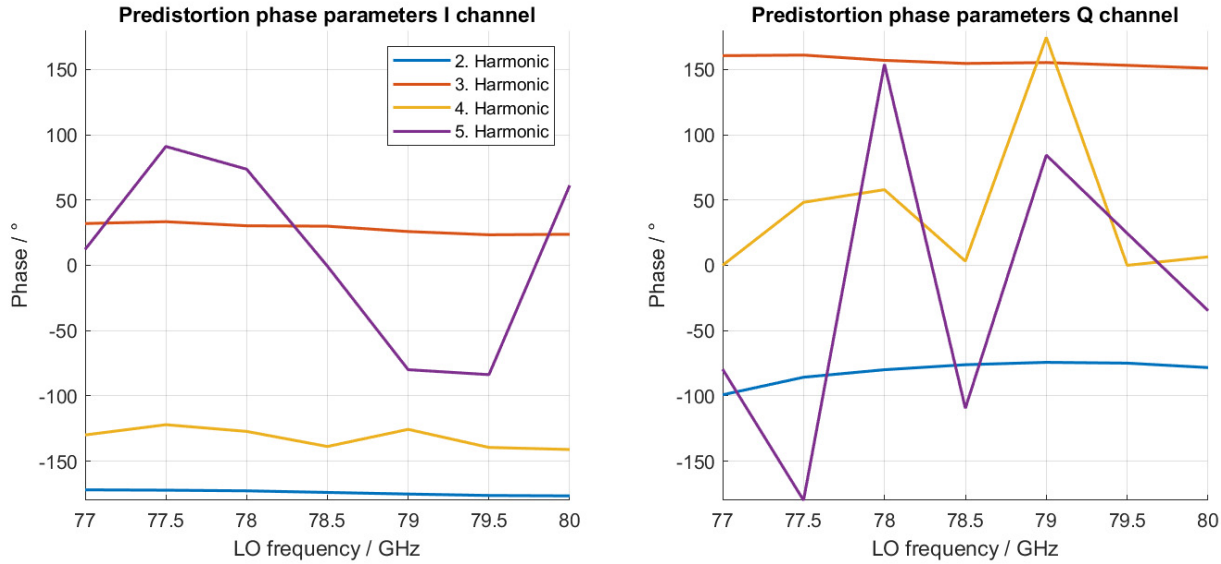

Figure 40: Phase for nonlinear predistortion for each harmonic over LO frequency

Figure 39 shows the different gains for each harmonic needed to perform the predistortion from (33) and (34) when the LO frequency is changed. Figure 40 shows the same but for the phase parameters. The biggest dependency on LO frequency can is observed for the linear phase correction shown in Figure 38. The nonlinear parameters stay more or less constant. The gain of the 4th and especially the 5th harmonic is very small or even zero. The phase of those signals jumps around with every measurement because if the amplitude is zero the phase does not matter. If it is nonzero but very small it is very hard to set the right phase because the impact on the output is very small. A good example is the 4th harmonic. On the I-input the needed signal is strong enough and the phase stays constant. On the Q-input the gain is barely above zero and the phase jumps with every measurement.

Applying the parameters extracted by this optimization process it is now possible to create an IF signal for the Mixer that shifts a given LO frequency down by a given IF frequency as required to stimulate the Radar chip.

4.7. Radar measurement

The Radar measurements presented in this section were accomplished on a test bench with a fully integrated radar chip from Infineon Technologies. The detailed specification of the chip as well as its settings and mode of operation are subject to confidentiality. Due to this reason, in the results shown in Figure 42 and Figure 44 the bottom of each Range Doppler map was cut off exactly 45 dB bellow the main signal peak.

As a baseline measurement, the Radar chip mentioned before was connected to a commercially available (fully featured) Radar Target Stimulator (RTS) using the setup highlighted in Figure 41.

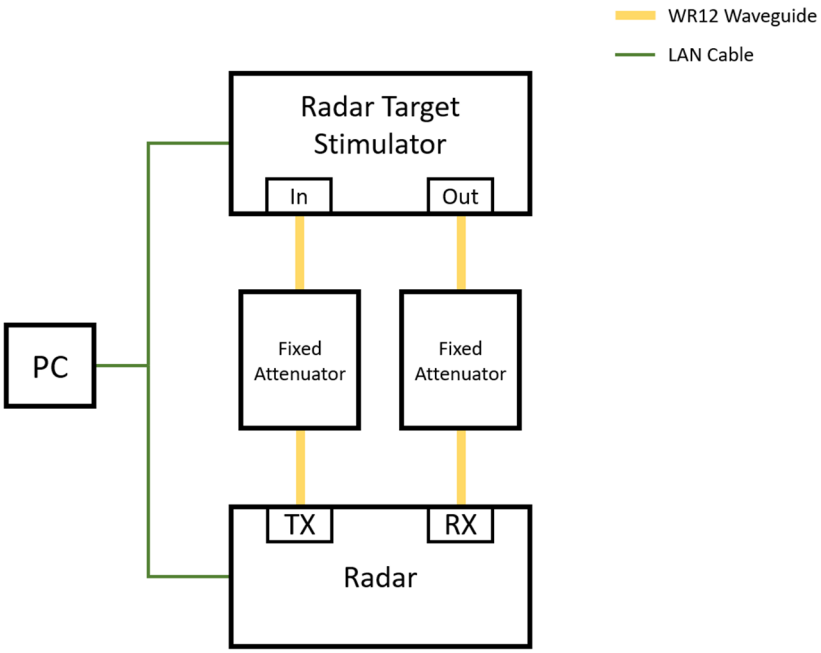

Figure 41: Block diagram of the Radar Target Stimulator setup

The fixed attenuator at the TX path reduced the output power of the radar to a level the RTS can safely handle. The attenuator in the RX path is applied in conjunction with the TX attenuator to give a high baseline attenuation for the whole system. The radar is built to function with antennas over the air and has to cope with the rather high losses cause by the free space propagation of the radiated signals. The baseline attenuation is used to roughly emulate this free space loss. The RTS itself supports fine tuning of the signal strength by adding additional attenuation. The Radar is configured to send out a specific number of chirps with a given centre frequency, bandwidth, chirp duration and fly back time. The same settings will be used for the IQ Mixer-based measurements as well. The target distance was chosen so that the radar beat frequency results in a 1 MHz signal. No Doppler shift is applied so the target is at zero velocity. The attenuation of the RTS was set in a way that the signal is a couple dBs below the clipping point of the radar input. The resulting range Doppler map looks very clean, as indicated in Figure 42.

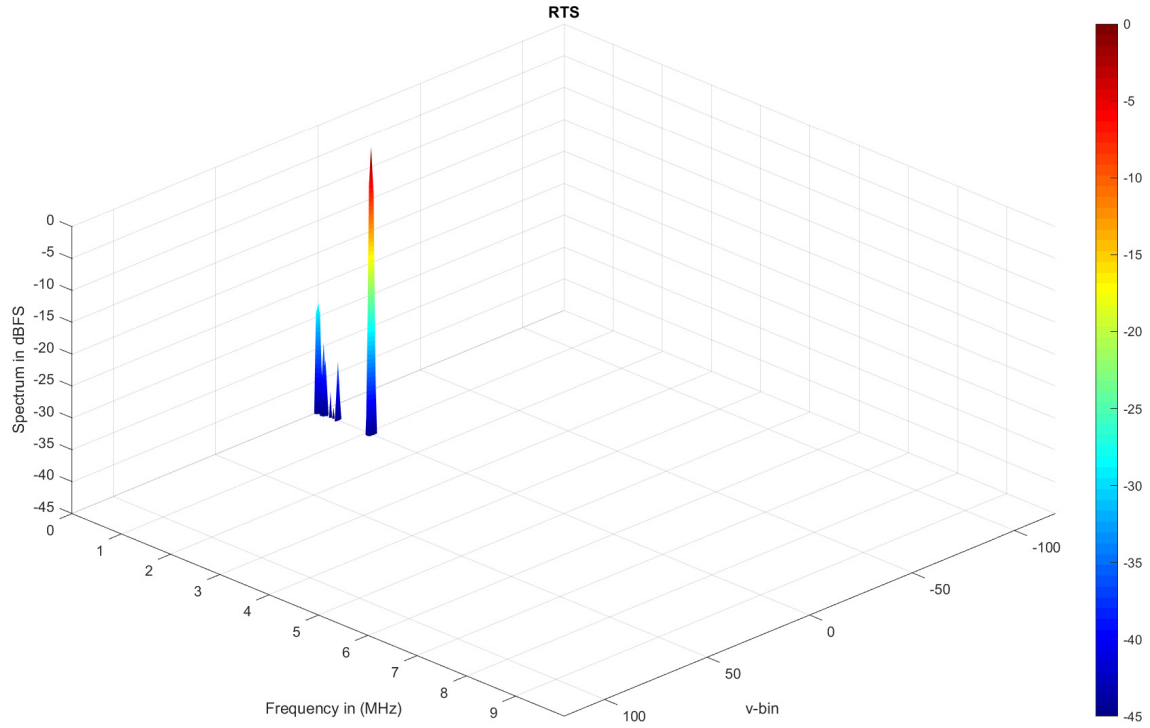

Figure 42: Range Doppler Map with a Radar Target Stimulator

The result shows only the Blocker with some close in reflections in the setup and the target at 1 MHz with no velocity (see Chapter 2.7).

Now the RTS is replaced by the Mixer. The measurement setup is summarized in Figure 43. For this measurement a waveguide directional coupler provides the input signal to the Radar chip. At the same time, the IQ-Mixer output signal is connected to the harmonic Mixer of the spectrum analyser.

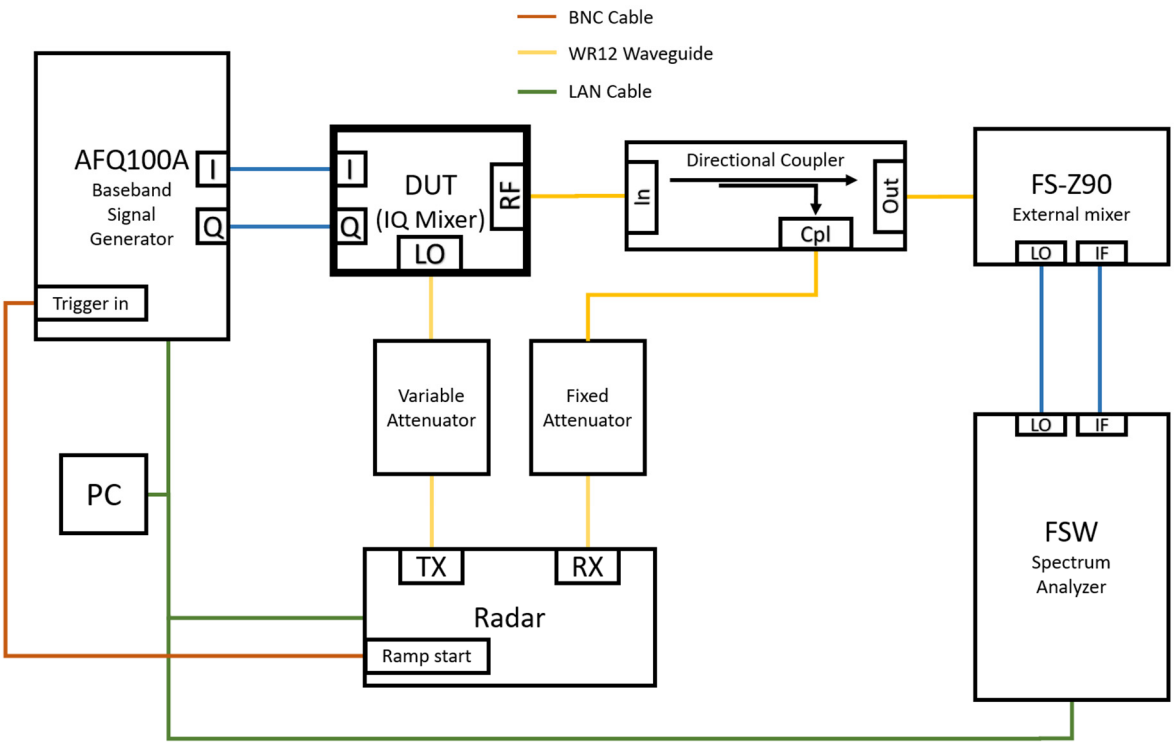

Figure 43: Block diagram of the Radar measurement with the IQ-Mixer

The attenuator between the TX output of the Radar and the LO input of the Mixer is adjustable. This is important because the LO input of the Mixer needs the same 8 dBm input level from the radar as in all the previous measurements. Since the Mixer is only compensated for this one power level at all LO frequencies it is necessary that the Radar can also keep this power level at all frequencies. This was checked before and the flatness of the output level from the radar is sufficient. If the power changes too much during one ramp of the Radar the Mixer will only be compensated for a small part of the ramp. This will result again in harmonic distortions and will be seen in the result. At the output of the IQ-Mixer a directional coupler is used to split the signal. The coupled port is used to add additional attenuation and feeds the signal back into the receiver of the Radar. The direct port of the coupler is connected to a FS-Z90 and spectrum analyser. To get the needed power level of 8 dBm into the Mixer the radar is put into a special continuous wave (CW) mode. In this mode it outputs only a single frequency carrier. With the help of the spectrum analyser connected to the Mixers' output I can monitor the undesired signal component created by the mixing process. By adjusting the variable attenuator connected to the LO input the power can be optimized to achieve the same low distortion level as documented in the last section. If it shows too much harmonic content the input level is either too high or too low. The level of the wanted lower sideband can also be used as a good indicator since it needs to be the same as in all the previous measurement results. The second attenuator placed before the receiver input of the Radar chip has a fixed value and reduces to signal to an appropriate level. Another very important connection between the Radar and the AFQ is needed. The Radar and the AFQ have both an independent reference oscillator. This means that 1 MHz generated by the AFQ will not be exactly measured as 1 MHz by the Radar. Hence, without any synchronisation a deviation in their frequencies for up to 10 kHz are expectable. This aspect itself is not a big problem but it also means that the starting phase of each radar chirp will change. This is equivalent to a

Doppler shift which is an undesired effect for the specified measurement. To circumvent this problem a special trigger from the Radar is used and fed into the AFQ. The Radar will pulse this trigger with the start of each new ramp and the AFQ will then start to output the computed IF signal. With this trigger the signal to the IQ Mixer always starts at the same defined phase for each ramp.

5. Result

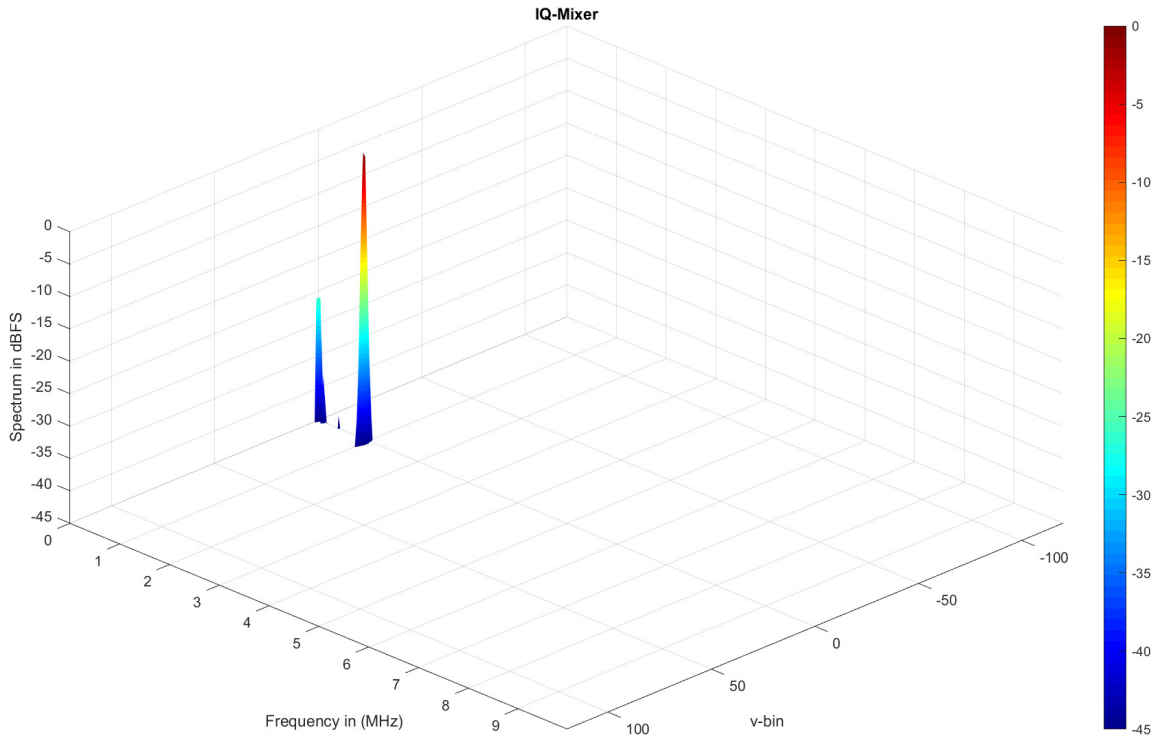

Figure 44: Range Doppler map with the IQ-Mixer setup

The resulting Range Doppler Map looks very impressive at this scale. The magnitude of the blocker is similar to the baseline measurement. The peak of the main target itself is at 1 MHz but has a very slight Doppler shift of one velocity bin and is a bit wider in the Doppler plane. This is probably caused by a slight jitter in the trigger of the AFQ. Also, no additional harmonic peaks are visible. Since the Radar is capable of a much higher dynamic range than shown here the harmonics of the Mixer start to appear at around the same level is on all CW measurements before. A RTS produces a much cleaner signal with a smooth noise floor. The IQ-Mixer however is still able to produce 55 dB of SFDR which shows that the applied predistortion also works when the Radar is ramping and not just in CW mode.

6. Limitations

The limitation of the machine learning approach is that the results are only valid for a very narrow band of input variables. Changing the IF or LO frequency is only possible within the measured range. The biggest and most important input variable is the input power of the LO. If it changes by only 1 dB the performance suffers significantly and all the parameter optimizations need to be run again. This limits the practical usability by a lot.

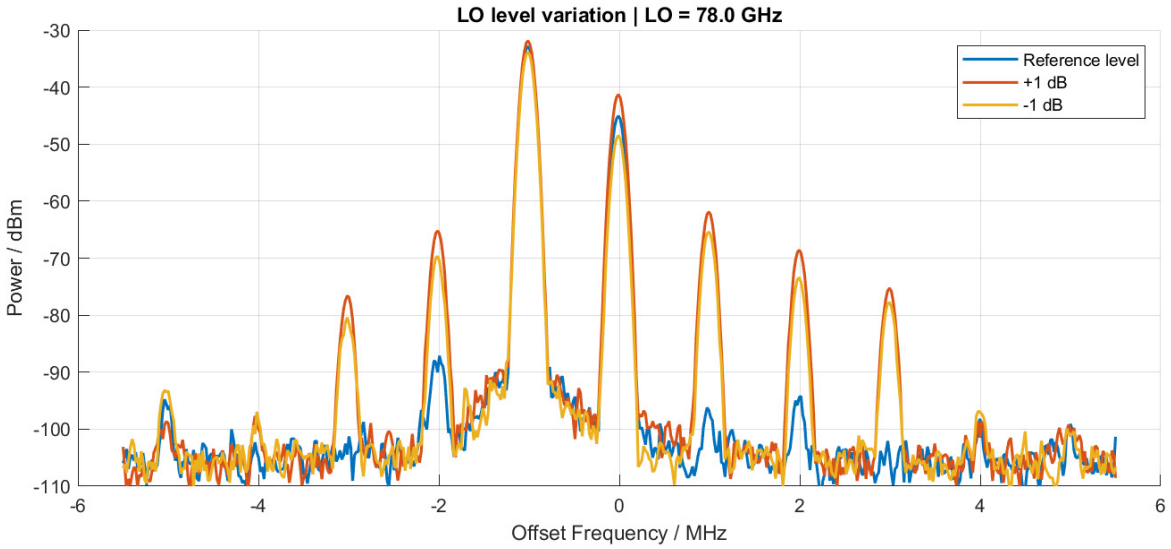

Figure 45: Harmonic rejection degradation with different LO power levels

7. Conclusion

The goal to stimulate a target on a modern automotive FMCW Radar using only an IQ-Mixer in the signal path of the Radar was reached. To achieve this with a performance of 55 dB spurious free dynamic range, it was necessary to predistort the input signal of the IQ-Mixer. The behaviour of the Mixer was too complicated for a simple diode-based model but an artificial intelligence based algorithm was able to find a solution. The usability of this solution is limited by a couple of factors described in Chapter 6 but as long as those limitations are not violated the performance (Figure 44) is close to the commercially available solution (Figure 42) used as reference for this thesis.

7.1. Possible improvements

The limiting factor for the predistortion in this setup is the dynamic range of the AFQ. A signal generator with a higher resolution digital to analogue converter would make an even higher SFDR possible. The setup could also be simplified by using the Radar itself as the signal source for all the measurements. The setup from Figure 43 would be perfectly capable to do so. This would also eliminate different LO power levels between two setups and would even account for slight shifts of the output power over the wanted frequency range. The time needed for all the machine learning optimisations can also be improved by using the previously found results as a starting point instead of always starting from zero since the parameters don't change a lot over frequency.

7.2. Future applications and next steps

With the generator in the first setup this method of predistortion can be used to generate also more complex signal instead of just shifting a single tone by a given frequency. As long as a metric like the SFDR can be specified the machine learning optimizer can work.

Another big topic would be the generation of a more complex IF signal for the Radar to test advanced radar signal processing like applying a micro Doppler to simulate rotating wheels on a car. Features like this are very complex to implement even with modern FPGA based Radar Target Stimulators or even impossible if the RTS is built on analogue principles.

The next steps of this project would be to try and derive a model from all the found solutions but this in itself would be another thesis.

8. Literature

[1] E. R. T. R. A. C. (ERTRAC), “Automated Driving Roadmap, 2017”.

[2] ECSEL Austria, “Austrian Research, Development & Innovation Roadmap for Automated Vehicles, ECSEL Europe, Vienna, 2016”.

[3] H. H. M. a. J. Dickmann, “Automotive Radar: From Its Origins to Future Directions, Microwave Journal, no. 9, 2013”.

[4] H. Meikle, Modern Radar Systems, 2nd ed., Artech House, 2008.

[5] C. Schyr, “"DrivingCube—A novel concept for validation of powertrain and steering systems with automated driving functions," in International Symposium on advanced vehicle control, 2013”.

[6] Keysight Technologies, “E8718A Radar Target Simulator, 76-81 GHz, with Remote Front End, 2020”.

[7] R. Collin, Foundations for Microwave Engineering, 2nd ed., McGrawHill, 1992.

[8] A. B. a. D. Horelick, A simple diode model including conductivity modulation, in IEEE Transactions on Circuit Theory, vol. 18, no. 2, pp. 233-240, March 1971.

[9] Marki Microwave,inc, IQ, IMAGE REJECT & single sideband Mixer Primer, https://www.markimicrowave.com/assets/appnotes/IQ_IR_SSB_Mixer_Primer.pdf from 15.01.2021.

[10] M. E. Gadringer, W. Bosch and G. Magerl, Phase Dependent Distortion in Direct Conversion Transmitters, in IEEE Transactions on Microwave Theory and Techniques, vol. 59, no. 12, pp. 3219-3227, 2011.

[11] C. S. a. G. M. M. E. Gadringer, Characterization and Modeling of Direct Conversion Transmitters, 2008 38th European Microwave Conference, Amsterdam, 2008.

[12] J. A. S. W. A. H. M. A. Richards, Principles of Modern Radar, Vol. 1 – Basic Principles, 2010: Scitech Publishing.

[13] S. M. S. I. V. Komarov, Fundamentals of Short-range FM Radar, Artech House, 2003.

[14] C. N. A. I. A. C. a. I. N. A. Macaveiu, A method for building the range-Doppler map for multiple automotive radar targets, 2014 11th International Symposium on Electronics and Telecommunications (ISETC), Timisoara, 2014.

[15] Sage millimeter, SFQ-60390315-1212SF-E1-M E-Band Quadrature Mixer Datasheet, https://sftp.eravant.com/content/datasheets/SFQ-60390315-1212SF-E1-M.pdf, opened 15.01.2021.

[16] M. E. Gadringer, Modeling and Compensation of Direct ConversionTransmitters and Receivers, Dissertation, 2011.

[17] H. Chernoff, A Note on the Inversion of Power Series. Mathematical Tables and Other Aids to Computation, 1947.

[18] R. a. P. K. Storn, Differential evolution - a simple and efficient heuristic for global optimization over continuous spaces. Journal of Global Optimization. 11 : 341–359, 1997.

[19] T. F. a. G. M. M. E. Gadringer, Comparison of the imbalance effects in direct conversion transmitters and receivers, 2011 Workshop on Integrated Nonlinear Microwave and Millimetre-Wave Circuits, Vienna, 2011.